Mon. Not. R. Astron. Soc. **000**, 1–?? (2005) Printed 18 July 2006 (MN LATEX style file v2.2)

Numerical simulations on the relative importance of starbursts and AGN in ultra-luminous infrared galaxies

Kenji Bekki[1⋆], Yasuhiro Shioya[2], and Matthew Whiting[3]

[1] *School of Physics, University of New South Wales, Sydney 2052, NSW, Australia*

[2] *Physics Department, Graduate School of Science and Engineering, Ehime University, 2-5 Bunkyo-cho, Matsuyama, Ehime 790-8577, Japan*

[3] *Australia Telescope National Facility, CSIRO, P.O. Box 76, Epping NSW 1710, Australia*

Accepted, Received 2005 February 20; in original form

ABSTRACT

We investigate the relative importance of starbursts and AGN in nuclear activities of ultra-luminous infrared galaxies (ULIRGs) based on chemodynamical simulations combined with spectrophotometric synthesis codes. We numerically investigate both the gas accretion rates ($\dot{m}_{\rm acc}$) onto super massive black holes (SMBHs) and the star formation rates ($\dot{m}_{\rm sf}$) in ULIRGs formed by gas-rich galaxy mergers and thereby discuss what powers ULIRGs. Our principal results, which can be tested against observations, are as follows.

(1) ULIRGs powered by AGN can be formed by major merging between luminous, gas-rich disk galaxies with prominent bulges containing SMBHs, owing to the efficient gas fuelling ($\dot{m}_{\rm acc} > 1{\rm M}_{\odot}$ yr^{-1}) of the SMBHs. AGN in these ULIRGs can be surrounded by compact poststarburst stellar populations (e.g., A-type stars).

(2) ULIRGs powered by starbursts with $\dot{m}_{\rm sf} \sim 100{\rm M}_{\odot}$ yr^{-1} can be formed by merging between gas-rich disk galaxies with small bulges having the bulge-to-disk-ratio ($f_{\rm b}$) as small as 0.1.

(3) The relative importance of starbursts and AGN can depend on physical properties of merger progenitor disks, such as $f_{\rm b}$, gas mass fraction, and total masses. For example, more massive galaxy mergers are more likely to become AGN-dominated ULIRGs.

(4) For most models, major mergers can become ULIRGs, powered either by starbursts or by AGN, only when the two bulges finally merge. Interacting disk galaxies can become ULIRGs with well separated two cores ($>$ 20kpc) at their pericenter when they are very massive and have small bulges.

(5) Irrespective of the choice of model, interacting/merging galaxies show the highest accretion rates onto the central SMBHs, and the resultant rapid growth of the SMBHs occur when their star formation rates are very high.

Based on these results, we discuss an evolutionary link between ULIRGs, QSOs with poststarburst populations, and "E+A" galaxies. We also discuss spectroscopic properties (e.g., Hβ luminosities and line ratio of [O III]/Hβ) in galaxy mergers with starbursts and AGN.

Key words: galaxies: active– galaxies: starbursts – galaxies: nuclei – galaxies: interactions – (galaxies): quasars: general

1 INTRODUCTION

The observation that ultra-luminous infrared galaxies (ULIRGs, defined as those with infrared luminosities greater than 10^{12} $L_{\odot}$) show a mixture of two distinct types of nuclear activities, namely starbursts and active galactic nuclei (AGN), has led to many observational studies of their formation and evolution processes (e.g., Sanders et al. 1988; Solomon et al. 1992; Soifer et al. 1986; Clements et al. 1996; Murphy et al. 1996; Sanders & Mirabel 1996; Gao & Solomon 1999; Trentham et al. 1999; Veilleux et al. 1999; Scoville et al. 2000; Surace et al. 2000; Bushouse et al. 2002;

⋆ E-mail: bekki@bat.phys.unsw.edu.au

Tacconi et al. 2002; Farrah et al. 2003; Armus et al. 2004; Imanishi & Terashima 2004; Colina et al. 2005; Iwasawa et al. 2005). For example, Sanders et al. (1988) proposed that ULIRGs formed by gas-rich galaxy mergers can finally evolve into QSOs after the removal of dust surrounding QSO black holes. Spectroscopic properties of ULIRGs have been extensively discussed in terms of the relative importance of starbursts and active galactic nuclei (AGN) in the energy budget of ultra-luminous infrared galaxies (e.g., Genzel et al. 1998; Lutz et al. 1998).

These observations have so far raised many questions, the most significant being: (1) whether all ULIRGs evolve into QSOs, (2) what mechanisms are responsible for triggering starbursts and AGN obscured heavily by dust in ULIRGs, (3) what determines the relative importance of starbursts and AGN in spectral energy distributions (SEDs) of ULIRGs, (4) whether there is an evolutionary link between starbursts and AGN in ULIRGs, and (5) whether there can be physical relationships between low redshift (low-z) ULIRGs and high-z dust-enshrouded starbursts and AGN at intermediate and high redshifts recently revealed by SCUBA (Submillimeter Common-User Bolometer Array) (e.g., Barger et al. 1998; Smail et al. 1997, 1998, 1999; Blain et al. 1999). Morphological studies of ULIRGs revealed that they show strongly disturbed morphologies indicative of violent galaxy interaction and merging. Previous theoretical studies have tried to answer the above five questions in the context of gas fuelling to the central region of galaxy mergers (See Shlosman et al. 1990 for more general discussions on fuelling mechanism in galaxies).

Physical mechanisms responsible for the formation of starbursts in galaxy mergers have been investigated by many authors (e.g., Olson & Kwan 1990; Barnes & Hernquist 1991; Noguchi 1991; Mihos & Hernquist 1994, 1996; Gerritsen & Icke 1997). For example, Olson & Kwan (1990) suggested that high velocity disruptive cloud-cloud collisions, which are more prominently enhanced in mergers, are responsible for the observed high star formation rates in galaxy mergers. Although these previous numerical studies provided some theoretical predictions on star formation rates (SFRs) and their dependence on the initial physical parameters of galaxy merging (e.g., bulge-to-disk-ratio and gas mass fraction), they did not investigate both SFRs and accretion rates (ARs) onto the central super-massive black holes (SMBHs) simultaneously. Therefore, they did not provide useful theoretical predictions on the formation and evolution of AGN, or on a possible evolutionary link between starbursts and AGN in ULIRGs.

Physical processes of gas fuelling to the central SMBHs in galaxy mergers have been investigated by a number of authors (Bekki & Noguchi 1994; Bekki 1995; Di Matteo et al. 2005; Springel et al. 2005a, b). Using dynamical simulations with rather idealized modeling of gas dynamics and star formation, Bekki & Noguchi (1994) first investigated both SFRs and ARs in merging galaxies and found that SFRs become very high at the epoch of the coalescence of the cores of two merging galaxies, whereas ARs attain their maxima only after the coalescence. Recently, Springel et al (2005a) have performed more sophisticated, high-resolution SPH simulations including feedback effects of AGN on the interstellar medium (ISM), and thereby demonstrated that AGN feedback can be quite important for global photometric properties of elliptical galaxies formed by major galaxy merging. These previous models however did not discuss the latest observational results of ULIRGs, partly because their model do not allow authors to investigate photometric and spectroscopic properties of dusty starbursts and AGNs in galaxy mergers.

The purpose of this paper is thus to investigate simultaneously both SFRs and ARs of merging galaxies in an self-consistent manner and thereby try to address the aforementioned questions related to the origin of ULIRGs. We particularly try to understand (1) physical conditions required for galaxy mergers to evolve into ULIRG with AGN (or starbursts), (2) key factors which determine the relative importance of starbursts and AGN, and (3) epochs when mergers become ULIRGs with AGN. We develop a new model in which the physics of star formation (including gas consumption and supernovae feedback by star formation), the time evolution of accretion disks around SMBHs, and the growth of SMBHs via gas accretion from the accretion disks are included. By using this new model, we show (1) how SFRs and ARS in merging galaxies evolve with time, (2) how they depend on galactic masses, mass ratios of two merging spirals, and bulge-to-disk-ratios of the merger progenitor spirals, and (3) how SMBHs grow in the central regions of starbursting mergers. We also show emission line properties of galaxies with starbursts and AGNs by combining the results of the simulated SFRs and ARs with spectral evolution codes.

Although previous numerical simulations combined with spectrophotometric synthesis codes have already derived SEDs of *purely starburst* galaxies obscured by dust (Bekki et al. 1999; Bekki & Shioya 2000, 20001; Jonsson et al. 2005), they did not discuss at all the spectrophotometric properties of galaxies *where starbursts and AGN coexist*. Therefore our new way of deriving spectral properties based on simulation results enables us to answer some key questions raised by recent large, systematic survey of AGN (e.g., Kauffmann et al. 2003), such as why a significant fraction of high-luminosity AGN have the Balmer absorption lines. Previous one-zone spectroscopic models discussed what controls emission and absorption line properties of galaxies with starbursts and AGN (Baldwin, Phillips & Terlevich 1981; Veilleux & Osterbrock 1987; Kewley et al. 2001; Dopita et al. 2006). The present simulations allow us to discuss this point based on the results of SFRs and ARs derived by chemodynamical simulations with growth of SMBHs.

The plan of the paper is as follows: In the next section, we describe our numerical model for calculating SFRs and ARs in merging galaxies. In §3, we present the numerical results on the time evolution of SFRs and ARs and its dependences of model parameters. In this section, we also show emission line properties of galaxies mergers with starbursts and AGN. We discuss the present results in terms of formation and evolution of ULIRGs and QSOs in §4. We summarise our conclusions in §5.

2 THE MODEL

Since the numerical methods and techniques we employ for modeling the chemodynamical and photometric evolution of galaxy mergers have already been described in detail else-

Table 1. Model parameters

Model no.	M_d ($\times 10^{10}$M$_\odot$)	$f_{\rm g}{}^a$	$f_{\rm b}{}^b$	$m_2{}^c$	orbital type	$m_{\rm sf,max}{}^d$	$m_{\rm acc,max}{}^e$	Comments
M1	6.0	0.2	0.5	1.0	FI	2.6×10^0	2.5×10^0	standard
M2	6.0	0.2	0.5	1.0	FI	6.4×10^2	0×10^0	no accretion onto SMBHs
M3	0.15	0.2	0.5	1.0	FI	1.3×10^{-1}	4.0×10^{-4}	
M4	3.0	0.2	0.5	1.0	FI	5.0×10^0	7.0×10^{-1}	
M5	30.0	0.2	0.5	1.0	FI	3.0×10^2	9.2×10^1	
M6	0.15	0.2	0.1	1.0	FI	2.1×10^{-1}	6.9×10^{-5}	
M7	3.0	0.2	0.1	1.0	FI	5.1×10^0	8.2×10^{-3}	
M8	6.0	0.2	0.1	1.0	FI	9.5×10^0	3.0×10^{-2}	
M9	30.0	0.2	0.1	1.0	FI	9.8×10^1	9.5×10^{-1}	
M10	6.0	0.2	0.5	1.0	HI	2.2×10^1	2.3×10^0	
M11	6.0	0.2	0.5	1.0	RR	2.2×10^1	3.6×10^0	
M12	6.0	0.2	0.5	1.0	BO	3.3×10^1	4.1×10^0	
M13	6.0	0.2	0.5	0.1	BO	6.0×10^0	1.0×10^{-2}	LSB minor merger
M14	6.0	0.2	0.5	0.3	BO	6.8×10^0	1.0×10^{-1}	unequal-mass merger
M15	6.0	0.2	0.5	0.1	BO	8.5×10^0	2.0×10^{-1}	HSB minor merger
M16	6.0	0.02	0.5	1.0	FI	6.8×10^{-1}	4.9×10^{-3}	gas poor
M17	6.0	0.05	0.5	1.0	FI	1.8×10^0	1.0×10^{-1}	
M18	6.0	0.1	0.5	1.0	FI	8.3×10^0	1.6×10^0	
M19	6.0	0.2	0.02	1.0	FI	1.1×10^2	2.9×10^{-3}	smaller bulge
M20	6.0	0.2	1.0	1.0	FI	6.0×10^1	1.6×10^0	bigger bulge
M21	6.0	0.05	1.0	1.0	FI	3.1×10^0	6.1×10^{-1}	bigger bulge, gas poor
M22	30.0	0.2	0.1	1.0	TI	5.7×10^1	2.4×10^0	tidal interaction

^{a} initial gas mass fraction
^{b} mass ratio of bulge to disk
^{c} mass ratio of merging two disks
^{d} maximum star formation rate (M$_\odot$ yr^{-1})
^{e} maximum accretion rate (M$_\odot$ yr^{-1})

where (Bekki & Shioya 1998, 1999), we give only a brief review here.

2.1 Progenitor disk galaxies

The progenitor disk galaxies that take part in a merger are taken to have a dark halo, a bulge, and a thin exponential disk. Their total mass and size are $M_{\rm d}$ and $R_{\rm d}$, respectively. From now on, all masses are measured in units of $M_{\rm d}$ and distances in units of $R_{\rm d}$, unless otherwise specified. Velocity and time are measured in units of $v = (GM_{\rm d}/R_{\rm d})^{1/2}$ and $t_{\rm dyn}$ $= (R_{\rm d}^3/GM_{\rm d})^{1/2}$, respectively, where G is the gravitational constant and assumed to be 1.0 in the present study. If we adopt $M_{\rm d} = 6.0 \times 10^{10}$ M$_\odot$ and $R_{\rm d} = 17.5$ kpc as fiducial values, then $v = 1.21 \times 10^2$ km s^{-1} and $t_{\rm dyn} = 1.41 \times 10^8$ yr.

We adopt the density distribution of the NFW halo (Navarro, Frenk & White 1996) suggested from CDM simulations:

$$\rho(r) = \frac{\rho_s}{(r/r_{\rm s})(1 + r/r_{\rm s})^2}, \quad (1)$$

where r, ρ_s, and $r_{\rm s}$ are the spherical radius, the characteristic density of a dark halo, and the scale length of the halo, respectively. The dark matter distribution is truncated at $r = 10r_{\rm s}$ corresponding to r_{200} in the NFW. The value of $r_{\rm s}$ (0.8) is chosen such that the rotation curve of the disk is reasonably consistent with observations. The bulge has a density profile with a shallow cusp (Hernquist 1990):

$$\rho(r) \propto r^{-1}(r + a_{\rm bulge})^{-3}, \quad (2)$$

where $a_{\rm bulge}$ is the scale length of the bulge. The ratio of a bulge mass ($M_{\rm b}$) to a disk mass ($M_{\rm d}$) in a disk is regarded as a free parameter and represented as $f_{\rm b}$. We determine the bulge scale length, $a_{\rm bulge}$, for a given $M_{\rm b}$ based on the Faber-Jackson relation (Faber & Jackson 1976) and the virial theorem. The bulge mass and its compactness can control the bar formation in the disks and thus the strength of starbursts in mergers. The bulge contains a SMBH with the mass ($M_{\rm SMBH}$) following the observed relation (Magorrian et al. 1998);

$$M_{\rm SMBH} = 0.006 M_{\rm b} = 0.006 f_{\rm b} M_{\rm d}. \quad (3)$$

The model for the time evolution of $M_{\rm SMBH}$ is described later.

The dark matter to disk mass ratio is fixed at 9 whereas the bulge to disk ratio is assumed to be a free parameter ($f_{\rm b}$). The radial (R) and vertical (Z) density profiles of the disk are assumed to be proportional to $\exp(-R/R_0)$ with scale length $R_0 = 0.2$ and to $\mathrm{sech}^2(Z/Z_0)$ with scale length $Z_0 = 0.04$ in our units, respectively. In addition to the rotational velocity attributable to the gravitational field of the disk and halo components, the initial radial and azimuthal velocity dispersions are added to the disk component in accordance with the epicyclic theory, and with a Toomre parameter value of $Q = 1.5$ (Binney & Tremaine 1987) . The vertical velocity dispersion at a given radius is set to be 0.5 times as large as the radial velocity dispersion at that point, as is consistent with the trend observed in the Milky Way (e.g., Wielen 1977).

The ratio of R_0 to R_d and that of $r_{\rm s}$ to R_0 are fixed at 0.2 and 4.0, respectively, for all disk models with different $M_{\rm d}$. Since we adopt the scaling relation of $\mu_s \propto {M_{\rm d}}^{0.5}$ (Kauff-

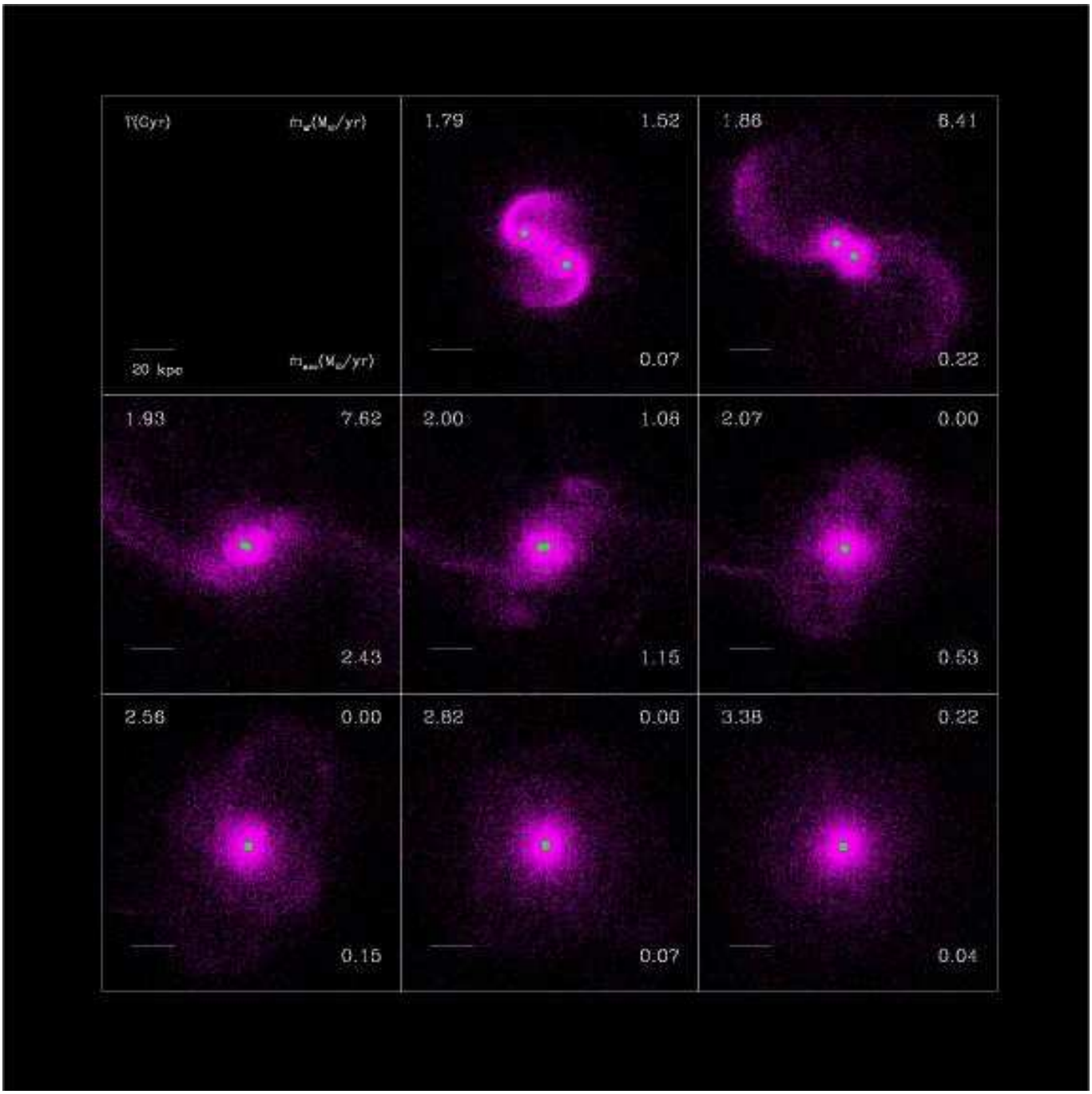

Figure 1. Mass distributions projected onto the x-y plane for the standard model. For convenience, stellar particles (old stars) and gaseous ones are shown in magenta (i.e. dark matter halo particles are not shown). Big green dots represent the locations of SMBH1 and 2. Time (T), SFRs ($\dot{m}_{\rm sf}$ in units of $\rm M_{\odot}yr^{-1}$), ARs ($\dot{m}_{\rm ac}$ in units of $\rm M_{\odot}yr^{-1}$) and the simulation scale are shown at upper left, upper right, lower right, and lower left, respectively, for each frame. Here time T represents the time that has elapsed since the simulation starts. Note that ARs can become very high ($> 1\rm M_{\odot}yr^{-1}$) when the two bulges finally merge (i.e. when the two SMBHs become very close with each other).

mann et al. 2003b), where μ_s is the mean stellar surface density of a disk (described later in 2.6), $R_{\rm d} = C_{\rm s} \times {M_{\rm d}}^{0.25}$ (or $R_0 \propto {M_{\rm d}}^{0.25}$). The normalization factor $C_{\rm s}$ is determined such that $R_0 = 3.5$ kpc for $M_{\rm d} = 6.0 \times 10^{10}$ $\rm M_{\odot}$. Thus the scale lengths of disks are different between models with different $M_{\rm d}$.

2.2 Star formation rates

The disk is composed both of gas and stars, with the gas mass fraction ($f_{\rm g}$) being a free parameter and the gas disk represented by a collection of discrete gas clouds that follow the observed mass-size relationship (Larson 1981). All overlapping pairs of gas clouds are made to collide with the same

restitution coefficient of 0.5 (Hausman & Roberts 1984). The gas is converted solely into field stars: we do not consider the formation of globular clusters (GCs). Field star formation is modeled by converting the collisional gas particles into collisionless new stellar particles according to the algorithm of star formation described below. We adopt the Schmidt law (Schmidt 1959) with exponent $\gamma = 1.5$ ($1.0 < \gamma < 2.0$, Kennicutt 1998) as the controlling parameter of the rate of star formation. The amount of gas consumed by star formation for each gas particle in each time step is given by:

$$\dot{\rho_{\rm g}} \propto {\rho_{\rm g}}^{\gamma}, \tag{4}$$

where $\rho_{\rm g}$ is the gas density around each gas particle. The coefficients in the law are taken from the work of Bekki (1998, 1999): The mean star formation rate in an isolated disk model with $M_{\rm d} = 6.0 \times 10^{10}$ $\rm M_{\odot}$ and the gas mass fraction of 0.1 for 1 Gyr evolution is ~ 1 $\rm M_{\odot}$ for the adopted coefficient (thus consistent with the observed star formation rate in the Galaxy; e.g., van den Bergh 2000). These field stars formed from gas are called "new stars" (or "young stars") whereas stars initially within a disk are called "old stars" throughout this paper. The adopted star formation model is similar to that with $C_{\rm SF} = 3.5$ in Bekki & Shioya (1998).

Chemical enrichment through star formation during galaxy merging is assumed to proceed both locally and instantaneously in the present study. We assign the metallicity of the original gas particles to the new stellar particles and increase the metallicity of the neighboring gas particles. The total number of neighboring gas particles is taken to be $N_{\rm gas}$, given by the following equation for chemical enrichment:

$$\Delta M_{\rm Z} = \{Z_i R_{\rm met} m_{\rm s} + (1.0 - R_{\rm met})(1.0 - Z_i) m_{\rm s} y_{\rm met}\}/N_{\rm gas}. \tag{5}$$

Here, $\Delta M_{\rm Z}$ represents the increase in metallicity for each gas particle, Z_i the metallicity of the new stellar particle (or that of the original gas particle), $R_{\rm met}$ the fraction of gas returned to the interstellar medium, $m_{\rm s}$ the mass of the new star, and $y_{\rm met}$ the chemical yield. The values of $R_{\rm met}$ and $y_{\rm met}$ are set to 0.3 and 0.02 respectively.

Using numerical simulations, Thornton et al. (1998) demonstrated that the total amount of energy that supernovae can give to the ISM ranges from $\approx 9 \times 10^{49}$ to $\approx 3 \times 10^{50}$ ergs with a typical case being $\approx 10^{50}$ ergs. This amount is roughly 10 % of the total amount of energy of Type II SN and 20 % of Type I (Thornton et al. 1998). They also found that most of the energy of supernovae can be in the form of kinetic energy within the ISM. Guided by these previous theoretical results, we assume that 10% of supernovae energy can be converted into kinematical energy of gas clouds. We adopt the Salpeter IMF with the lower mass cut off of 0.1 $\rm M_{\odot}$, the upper one of 100.0 $\rm M_{\odot}$ and the exponent of the slope equal to -2.35 (i.e. a canonical IMF). Total number of supernovae at each time step can be calculated according to the star formation rate. The more details of the numerical method to give kinematical energy of supernovae to gas clouds are given in Bekki & Shioya (1999).

2.3 Accretion rates onto SMBHs

AGN activity is believed to originate from sub-parsec size regions at the galactic nuclei, powered by the mass accretion onto SMBHs through accretion disks (e.g., Rees 1984). In the present study, we assume that SMBHs are not surrounded by accretion disks in initial disks and thus the accretion disks are assumed to form during merging. Therefore, we need to model (1) formation processes of accretion disks around SMBHs and (2) time evolution of ARs in growing accretion disks in order to estimate ARs in an self-consistent manner. Although numerous theoretical studies have already been made for physical properties of static accretion disks (e.g., Frank, King & Raine 2002), there have been no extensive theoretical studies on ARs in accretion disks that are *forming and growing* through radial gas inflow into the central sub-parsec-scale region of galaxies from their outer parts. Furthermore only a few theoretical attempts have been made to elucidate the formation process of gaseous tori and accretion disks around SMBHs (e.g., Bekki 2000).

Given this lack of theoretical detail on the evolution of accretion disks, we adopt the following two-fold model to calculate ARs. For each time step of a simulation, we first calculate total gas mass that can be used for the formation of an accretion disk around a SMBH in the central region of a galaxy by assuming that tidal interaction between the SMBH and its nearby gas clouds and the resultant destruction of gas clouds (Bekki 2000) can be responsible for gas supply to the accretion disk. Then, by using a reasonable analytical model, we calculate the time evolution of the AR ($\dot{m}_{\rm acc}$) onto the SMBH for a given mass of the accretion disk at each time step. The details of this two-fold model are described as follows.

2.3.1 Formation of an accretion disk around a SMBH

The mass of an accretion disk around a SMBH is assumed to increase as a result of gas accretion from gas clouds being gravitationally trapped and destroyed by the SMBH (Bekki 2000). We estimate the total mass of an accretion disk ($M_{\rm ad}$) around a SMBH based on gas densities of gas clouds within $R_{\rm acc}$ from the SMBH. We assume that gas clouds within $R_{\rm acc}$ can be used as fuel for an accretion disk. Bekki & Noguchi (1994) adopted $R_{\rm G}$ as $R_{\rm acc}$, where $R_{\rm G}$ is defined as

$$R_{\rm G} = \frac{G M_{\rm SMBH}}{\sigma^2} \tag{6}$$

where $M_{\rm SMBH}$ is the mass of the SMBH and σ is the velocity dispersion (or any characteristic velocity) in the background components, and G is the gravitational constant. This $R_{\rm G}$ can be estimated to be $\sim$ 10pc for $M_{\rm SMBH} = 10^8 \rm M_{\odot}$ in a canonical set of galaxy parameters (Bekki & Noguchi 1994).

Since our model for $M_{\rm ad}$ evolution is based on interaction between SMBHs and gas clouds, we adopt the "Bondi" radius ($R_{\rm B}$) rather than $R_{\rm G}$ as $R_{\rm acc}$. $R_{\rm B}$ is described as

$$R_{\rm B} = \frac{2 G M_{\rm SMBH}}{{v_{\rm rel}}^2} \tag{7}$$

where $v_{\rm rel}$ is relative velocity between the SMBH and gas. We assume that $v_{\rm rel}$ is equivalent to the central velocity dispersion of a bulge in each model. Therefore, $R_{\rm acc}$ is initially determined by the bulge mass of $M_{\rm b}$ ($= f_{\rm b} M_{\rm d}$) in a model owing to the adopted relation of $M_{\rm SMBH} = 0.006 M_{\rm b}$ relation.

Next we estimate total mass of gas clouds within $R_{\rm acc}$ and thereby derive a local gas density ($\rho_{\rm g}$) around a SMBH. Guided by theoretical predictions by Hoyle & Lyttleton

(1941), Bondi (1952), and Ruffert & Arnett (1994), we calculate the accretion disk from gas clouds ($\dot{m}_{\rm cl}$) as follows:

$$\dot{m}_{\rm cl} = C_{\rm B} \times \rho_{\rm g}, \tag{8}$$

where $C_{\rm B}$ is linearly proportional to ${M_{\rm SMBH}}^2$ and ${v_{\rm rel}}^{-3}$. $C_{\rm B}$ is therefore chosen according to $M_{\rm SMBH}$ and $M_{\rm b}$ (and hence $M_{\rm d}$ and $f_{\rm b}$) in each model. Time evolution of $M_{\rm ad}$ is determined by solving the following equation in terms of $\dot{m}_{\rm cl}$ and $\dot{m}_{\rm acc}$:

$$\dot{M}_{\rm ad} = \dot{m}_{\rm cl} - \dot{m}_{\rm acc}. \tag{9}$$

$\dot{m}_{\rm acc}$ represents the mass accretion rate onto a SMBH and we describe the way to estimate $\dot{m}_{\rm acc}$ later. Equation (9) thus means that if there is no supply of gas from outer part of a galaxy into the nuclear accretion disk, $M_{\rm ad}$ gradually decreases owing to consumption of gas within the disk.

2.3.2 Time evolution of accretion rates

Based on $M_{\rm ad}$, we estimate AR ($\dot{m}_{\rm acc}$) at each time step in a simulation. We adopt a gas-pressure dominated standard α-disk with the conversion rate of accreted mass to energy(ϵ) equal to 0.1 and follow the relation between $M_{\rm ad}$ and $\dot{m}_{\rm acc}$ for a given $M_{\rm SMBH}$ shown in Liu (2004):

$$\dot{m}_{\rm acc} = 0.1(\frac{M_{\rm ad}}{7.7 \times 10^7 {\rm M}_\odot})^{5/3} {\rm M}_\odot {\rm yr}^{-1}. \tag{10}$$

We assume that $\dot{m}_{\rm acc}$ should not exceed the Eddington accretion rate, which is described as:

$$\dot{m}_{\rm Edd} = 2.3(\frac{M_{\rm SMBH}}{10^8 {\rm M}_\odot}) {\rm M}_\odot {\rm yr}^{-1}. \tag{11}$$

Thus, if $\dot{m}_{\rm acc} > \dot{m}_{\rm Edd}$, $\dot{m}_{\rm acc}$ is set to be $\dot{m}_{\rm Edd}$ at every time step in all simulations.

As a result of gas accretion onto a SMBH, $M_{\rm SMBH}$ is time-dependent and its evolution is described as:

$$M_{\rm SMBH}(t + \Delta t) = M_{\rm SMBH}(t) + \dot{m}_{\rm acc} \times \Delta t, \tag{12}$$

where Δt is the time step width (corresponding to $0.01 t_{\rm dyn}$) in a simulation. We consider that 10% of the rest mass of accreted gas (i.e. $0.1 \dot{m}_{\rm acc} \Delta t$) can be converted into energy ($E_{\rm acc}$). Although some fraction of $E_{\rm acc}$ may well be used for thermally and dynamically heating the ISM in galaxy mergers, it is unclear what fraction ($f_{\rm agn}$) of $E_{\rm acc}$ can be returned back to the ISM through AGN feedback effects. Accordingly, we compromise by assuming that $f_{\rm agn} = 0.1$, the same value as that derived for supernovae feedback effects (Thornton et al. 1998).

The AGN feedback energy from a SMBH is assumed to be used for the increase of kinetic energy of gas particles around the SMBH. Therefore, $f_{\rm agn} E_{\rm acc}$ is equivalent to the sum of the increase in kinematical energy of gas particles at each time step. The methods to give a velocity perturbation (directed radially away from the SMBH) to each gas particle around the SMBH are the same as those for stellar feedback effects in Bekki & Shioya (1999). The present results depend on $f_{\rm agn}$ such that gas transfer to nuclei (thus nuclear star formation and AGN fueling) can be more strongly suppressed in the models with larger $f_{\rm agn}$. In this paper, we consider that the adopted value of 0.1 is reasonable, because this value is similar both to that in Springel et al. (2005a) with $f_{\rm agn} = 0.05$ (explaining some observations) and to that by Thornton et al. (1998) for kinetic feedback effects for supernovae.

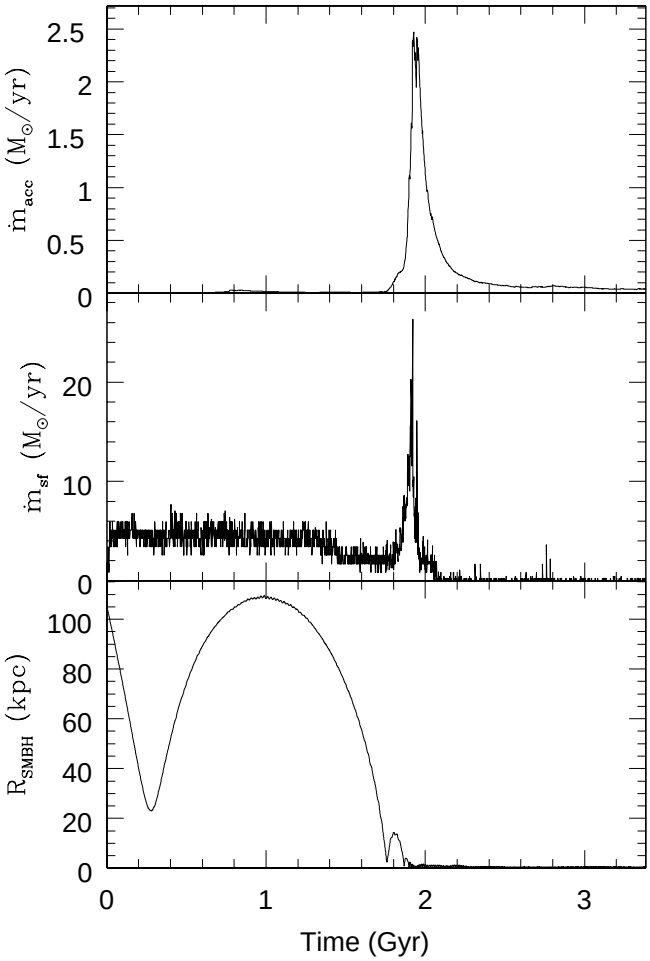

Figure 2. Time evolution of AR ($\dot{m}_{\rm acc}$; top), SFR ($\dot{m}_{\rm sf}$; middle), and separation of two SMBHs ($R_{\rm SMBH}$; bottom) in the standard model (M1). Note that the peak of the AR is nearly coincident with that of the SFR.

2.4 Orbital configurations

In all of the simulations of merging pairs, the orbit of the two disks is set to be initially in the xy plane and the distance between the center of mass of the two disks ($r_{\rm p}$) is assumed to be ten times the disk size. The pericenter distance and the eccentricity are set to be the disk size and 1.0 (i.e. parabolic), respectively, for most of the models. The spin of each galaxy in a merger is specified by two angles θ_i and ϕ_i, where suffix i is used to identify each galaxy. θ_i is the angle between the z axis and the vector of the angular momentum of a disk. ϕ_i is the azimuthal angle measured from the x axis to the projection of the angular momentum vector of a disk onto the xy plane.

We specifically present the results of the following three parabolic models with different disk inclinations with respect to the orbital plane: A fiducial model represented by "FI" with $\theta_1 = 0$, $\theta_2 = 30$, $\phi_1 = 0$, and $\phi_2 = 0$; a retrograde-retrograde model ("RR") with $\theta_1 = 180$, $\theta_2 = 210$, $\phi_1 = 0$, and $\phi_2 = 0$; and a highly inclined model ("HI") with $\theta_1 = 60$,

$\theta_2 = 60$, $\phi_1 = 90$, and $\phi_2 = 0$. In addition to these parabolic models with $e_{\rm p} = 1$, the bound orbit model ("BO") with the orbital eccentricity of 0.5 and with the same orbital configuration as the "FI" model is investigated. The time taken for the progenitor disks to completely merge and reach dynamical equilibrium is less than 16.0 in our units (~ 2.2 Gyr) for most of our major merger models.

In order to compare the time evolution of SFRs and ARs in mergers with that of tidally interacting galaxies, we investigate tidal interaction models ("TI"). Although we derive the results for several interaction models, we show only the most interesting case in the present study, since our main interest is on SFRs and ARs in galaxy mergers. We show a model with $e_{\rm p} = 1.1$ (i.e. hyperbolic), $\theta_1 = 0$, $\theta_2 = 30$, $\phi_1 = 0$, $\phi_2 = 0$ and $r_{\rm p}$ equal to 1.5 times the disk size. In the tidal interaction model, two disks do not merge at all and become separated from each other soon after their pericenter passage.

All the calculations related to the above chemodynamical evolution have been carried out on the GRAPE board (Sugimoto et al. 1990) at the Astronomical Data Analysis Center (ADAC) at the National Astronomical Observatory of Japan. The gravitational softening parameter was fixed at 0.025 in our units (0.44 kpc). The time integration of the equation of motion was performed by using the 2nd-order leap-frog method. Since the masses of the bulge particle are set to be the same in all simulations, the initial total particle number in each simulation depends on the bulge mass. The total particle numbers for dark matter halo, bulge, stellar disk, and gaseous one in a model with $f_{\rm b} = 1.0$ are 60000, 10000, 20000, 20000, respectively, in the present study.

2.5 Emission line properties

Our previous chemodynamical models with spectrophotometric synthesis codes for dusty starburst galaxies have already demonstrated that major mergers between gas-rich spirals can become ULIRGs with $L_{\rm ir} > 10^{12}{\rm L}_{\odot}$, because the triggered nuclear starburst components can be very heavily obscured by dust (Bekki et al. 1999; Bekki & Shioya 2000, 2001; Bekki et al. 2001). Since these previous studies have already described the details of evolution from galaxy mergers into ULIRGs, we here do not intend to discuss the formation processes of ULIRGs. We instead discuss optical emission properties of galaxy mergers with both starbursts and AGN based on SFRs and ARs derived from chemodynamical simulations. In the present paper, we discuss *global, averaged spectral properties* of galaxy mergers rather than the spatial difference of the properties. Two-dimensional distributions of emission line properties in ULIRGs will be discussed in our forthcoming papers (Bekki & Shioya 2005, in preparation).

We mainly demonstrate the time evolution of emission line properties of Hα, Hβ, [O III], and [NII] of galaxy mergers by considering the energy contribution from both thermal (i.e. starburst) and non-thermal (i.e. AGN) components. From the time evolution of $\dot{m}_{\rm sf}$ of a merger, we first derive the SED at each time step by using stellar population synthesis codes. This first step is exactly the same as that adopted in our previous one-zone chemo-photometric galaxy evolution models (Shioya & Bekki 1998; 2000; Shioya et al. 2001, 2002, 2004). Secondly, we derive the total luminosity of the Hβ line ($L_{\rm H\beta}$) from the production rate of ionizing photons based on the derived SED. Thirdly, by adopting a typical value of the Hα-to-Hβ ratio (i.e. Hα/H$\beta \sim 2.9$), and the observed values of [O III]/Hβ and [O III]/Hα in HII regions of nearby galaxies (Kennicutt et al. 1989), we derive $L_{\rm H\alpha}$, $L_{\rm [O\,III]}$, and $L_{\rm [N\,II]}$.

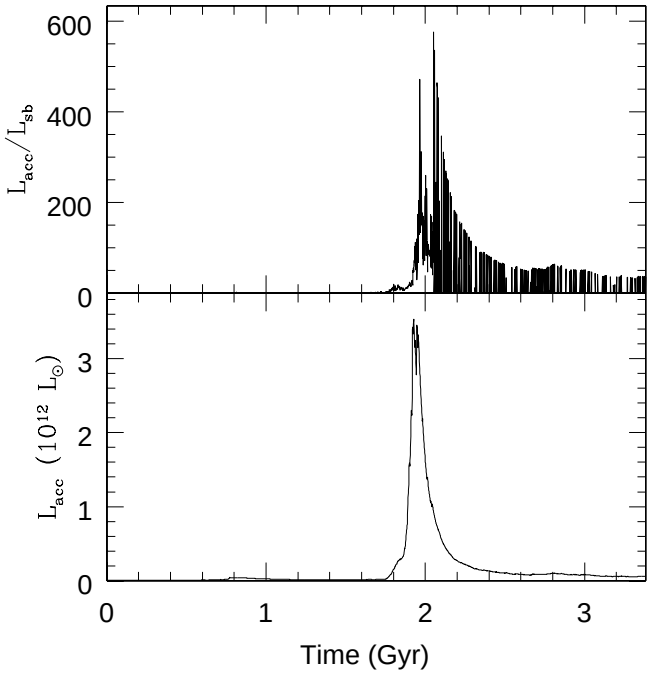

Figure 3. Time evolution of the ratio ($L_{\rm acc}/L_{\rm sf}$) of bolometric luminosity coming from AGN to that from starbursts (upper) and bolometric luminosity from AGN (lower) in the standard model (M1). Note that the time scale of the model to show the QSO-like luminosity ($> 10^{12}{\rm L}_{\odot}$) is quite short ($\sim$ 0.1Gyr). Note also that $L_{\rm acc}/L_{\rm sf}$ becomes higher (i.e. galactic nuclei dominated by accretion power induced activities) when $L_{\rm acc}$ becomes higher.

Fourthly, we calculate the bolometric luminosity ($L_{\rm bol}$) of AGN in the merger from the AR by assuming that the energy conversion efficiency (ϵ) in the accretion disk around a SMBH is 0.1. Fifthly, by adopting a reasonable set of values of $L_{\rm [O\,III]}/L_{\rm bol} = 1/300$, $L_{\rm [O\,III]}/L_{\rm x} = 0.01$, and $L_{\rm bol}/L_{\rm x} = 30$ (Kraemer et al. 2004), we calculate the $L_{\rm [O\,III]}$ value due to the AGN. Sixthly, we derive $L_{\rm H\alpha}$, $L_{\rm [O\,III]}$, and $L_{\rm [N\,II]}$. by adopting typical values of Hα/Hβ, [O III]/Hβ, and [O III]/Hα in nearby galaxies with Seyfert spectra (Kennicutt et al. 1989). Finally, we calculate the total luminosities of emission lines by combining the luminosities from starburst and AGN components. The effects of dust on spectroscopic properties of galaxy mergers model are not accounted for in the present model.

2.6 Main points of analysis

We mainly investigate SFRs and ARs and their dependences on model parameters of galaxy mergers. In order to clarify the relative importance of starbursts and accretion power induced activities in galactic nuclei, we estimate bolometric luminosities of starbursts (L_{sb}) and AGN ($L_{\rm acc}$) by using analytic formula. $L_{\rm sb}$ can be approximated as (Kennicut 1998):

$$L_{\rm sb} = 10^{12}(\frac{\dot{m}_{\rm sf}}{140{\rm M}_\odot{\rm yr}^{-1}}) \times (\frac{\eta_{\rm nuc}}{0.01}) \times (\frac{f_{\rm ys}}{0.05}){\rm L}_\odot, \quad (13)$$

where $\eta_{\rm nuc}$ is the energy conversion efficiency in nuclear fusion reactions (i.e. conversion of hydrogen to helium), and $f_{\rm ys}$ is the fraction of massive young stars in starbursts. $L_{\rm acc}$ can be approximated as (Shapiro & Teukolsky 1983; Frank et al 2002):

$$L_{\rm acc} = 10^{12}(\frac{\dot{m}_{\rm acc}}{0.7{\rm M}_\odot{\rm yr}^{-1}}) \times (\frac{\eta_{\rm acc}}{0.1}){\rm L}_\odot, \quad (14)$$

where $\eta_{\rm acc}$ is conversion efficiency of rest mass energy into radiation in accretion disks. These equations (13) and (14) clearly mean that for a galaxy to show a QSO-like luminosity ($\approx 10^{12}{\rm L}_\odot$), only small values of gas consumption rate ($0.7{\rm M}_\odot{\rm yr}^{-1}$) are required if the QSO-like luminosity originates from accretion powered activity.

We investigate SFRs, ARs, and emission line properties of galaxy mergers with starbursts and AGNs, and their dependences on initial disk masses ($M_{\rm d}$), bulge-to-disk-ratios ($f_{\rm b}$), gas mass fraction ($f_{\rm g}$), and mass ratios of two merging disks (m_2). For the models with different $M_{\rm d}$ and those with $m_2 \neq 1$, we need to change masses and sizes according to the scaling relation of galaxies. We adopt the observed scaling relation by Kauffmann et al. (2003b) and derive the following relation:

$$\mu_s \propto {M_{\rm d}}^{0.5}, \quad (15)$$

where μ_s is the mean stellar surface density of a disk. We determine $R_{\rm d}$ for a given $M_{\rm d}$ by using the equation (15) and the relation of $\mu_s \propto M_{\rm d}/{R_{\rm d}}^2$. The above scaling relation means that less luminous galaxies show lower surface brightness (LSB). For convenience, the model with $m_2 = 0.1$ (M13) including a smaller galaxy with the mass and the size consistent with the equation 12 is referred to as a "LSB minor merger". We also investigate a "HSB" minor merger model with $m_2 = 0.1$ (M15) in which a smaller galaxy has a surface brightness 2 mag higher than the LSB minor merger model.

We primarily show the results of the "standard" model M1, as this model shows typical behavior for the evolution of SFRs and ARs. Then we show the parameter dependences of other models. Below, we describe the results of 22 models and in Table 1 summarise the model parameters for these: Model number (column 1), total mass of a disk (2), the gas mass fraction (3), the mass ratio of bulge to disk (4), the mass ratio m_2 of two merging disks (5), orbital types (6), the maximum star formation rate (7), the maximum accretion rate (8), and comments on the models (9). In the following discussion, the time T represents the time that has elapsed since the simulation starts.

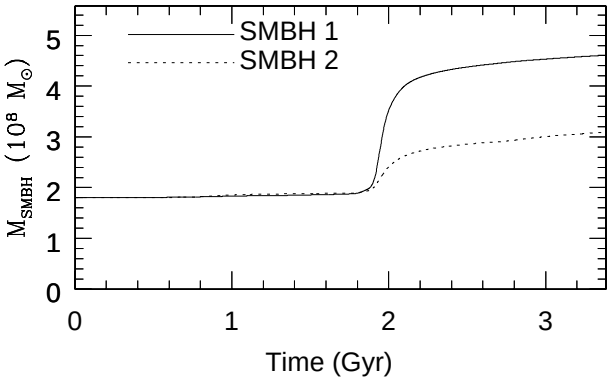

Figure 4. The time evolution of SMBH1 (solid) and SMBH2 (dotted) in the standard model.

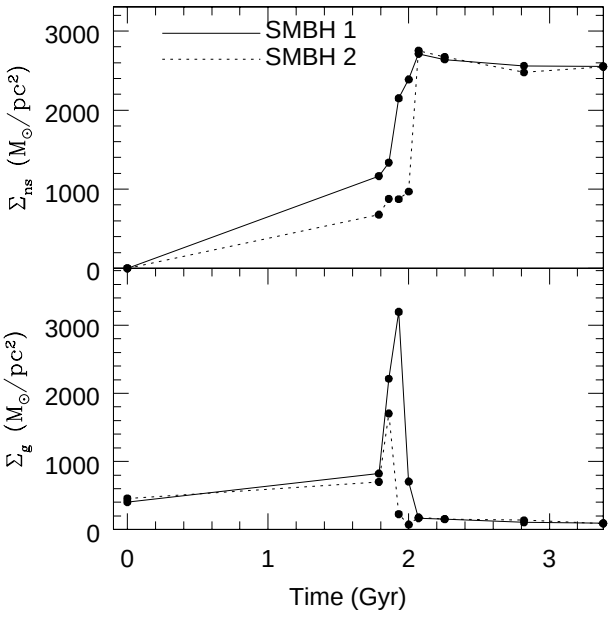

Figure 5. Time evolution of projected mass density ($\Sigma_{\rm ns}$) of new stars (i.e. poststarburst populations) around SMBH1 (solid) and 2 (dotted) of the merger (upper) and column gas density ($\Sigma_{\rm g}$) around the SMBHs (lower) in the standard model. For clarity and comparison, only the results at nine epochs shown in Figure 1 are described. The projected stellar density and column gas density are measured for particles that are located within 0.04 in simulation units (corresponding to 0.7 kpc) around SMBHs. The significantly increased values of $\Sigma_{\rm ns}$ after $T \sim 1.8$ Gyr mean that SMBHs are surrounded by compact poststarburst populations formed during galaxy merging. The very large values of $\Sigma_{\rm g}$ around $T = 1.9$ Gyr mean that SMBHs (thus AGN) are heavily obscured by metal-enriched gas (thus dust).

3 RESULTS

3.1 The standard model

3.1.1 Evolution of SFRs and ARs

Figure 1 illustrates the time evolution of morphological properties, SFRs, and ARs simultaneously for the galaxy merger in the standard model. The SFR can be moderately high ($\dot{m}_{\rm sf} \sim 6.4{\rm M}_\odot{\rm yr}^{-1}$) at $T = 1.86$ Gyr when two disks can be still clearly seen as separate entities, whereas the AR becomes very high ($\dot{m}_{\rm acc} > 1{\rm M}_\odot{\rm yr}^{-1}$) at $T = 1.93 - 2.00$ Gyr when two disks finally merge to form a giant elliptical galaxy. A disturbed outer morphology can be still seen at $T = 2.07$ and 2.56 Gyr when the AR becomes lower (i.e. weak AGN phases). Both the SFR and the AR become significantly low at $T = 2.82$ and 3.38 Gyr when the merger remnant can be morphologically identified as an elliptical with no peculiar fine structures (e.g., shells and plumes).

As Figure 2 reveals, showing the time evolution of SFR and AR in the standard model M1, both SFR and AR can

be maximised when the two SMBHs become close to each other. This is essentially because efficient radial transfer of gas into the central $10-100$pc in the merger occurs during the coalescence of the two big bulges. The AR exceeds the $0.7\mathrm{M}_{\odot}\mathrm{yr}^{-1}$ required for QSO activity ($L_{\rm bol} > 10^{12}\mathrm{L}_{\odot}$) at $T = 1.9 \sim 2.0$ Gyr whereas the SFR does not exceed the $100\mathrm{M}_{\odot}\mathrm{yr}^{-1}$ required to produce a QSO luminosity. Therefore, this merger can be regarded as a QSO dominated by activities induced by accretion power of SMBHs. The epoch of maximum AR nearly coincides with that of maximum SFR, and this coincidence can be seen in most of the present models. These results imply that (1) galaxy mergers with AGN activity can contain starburst components, and (2) starburst components in the merger would not be so easily detected owing to the overwhelming light from the AGN. Since morphological transformation from spirals into an elliptical is nearly finished at the epoch of the maximum AR in this model, the merger can be regarded as a forming elliptical with starburst and AGN components.

As a natural result of the high ARs in the galactic nuclei, the ratio of bolometric luminosity from the AGN ($L_{\rm acc}$) and that from the starburst ($L_{\rm sb}$) becomes very large in the final phase of galaxy merging. Figure 3 shows that (1) $L_{\rm acc}/L_{\rm sb}$ becomes higher as $L_{\rm acc}$ becomes higher, (2) it becomes more than 100 at the epoch of maximum $L_{\rm acc}$, and (3) it is higher during and after the coalescence of two disk galaxies than before. These results suggest that the central starburst component in a merger can be more difficult to detect when the AR of the merger becomes higher. They also suggest that young elliptical galaxies formed by major galaxy merging are more likely to show spectra with AGN features than HII region features. We will discuss this point in §4.1.

A key factor in the evolution of these systems is the presence of feedback from the AGN. If we construct a model that has gas consumption by SMBHs, but without AGN feedback, we find that the maximum $\dot{m}_{\rm sf}$ and $\dot{m}_{\rm acc}$ are increased by factors of 2.8 and 113.0 respectively compared to model M1 (which has the feedback present). This model also shows a higher residual star formation rate ($\dot{m}_{\rm sf} \sim 10\mathrm{M}_{\odot}\mathrm{yr}^{-1}$) in a sporadic way even after coalescence of two cores in galaxy merging. It is therefore clear from these results that (1) AGN feedback can suppress both (i) gas fueling to SMBHs and (ii) nuclear starbursts and (2) AGN feedback can strongly suppress residual star formation after coalescence of two cores. Springel et al. (2005b) have already pointed out that AGN feedback can expel the remaining gas from merger remnants to shut off star formation in their sophisticated models of AGN feedback. The self-control of the growth of the SMBH by AGN feedback effects may be important for better understanding the origin of the Magorrian relation (eg. Magorrian et al 1998). However, such discussion is outside the scope of this paper.

Figure 4 shows the time evolution of $M_{\rm SMBH}$ initially within bulges of the two merging disks. Both SMBHs grow quickly by a significant factor owing to efficient gas fuelling to the central $10-100$ pc and the resultant formation of massive accretion disks around them when star formation rates are quite high ($> 10\mathrm{M}_{\odot}\mathrm{yr}^{-1}$). The difference in the growth rates shown in Figure 2 is due to the fact that gas fuelling in the less inclined disk galaxy (i.e. galaxy 1) is more efficient than in the more inclined one (i.e. galaxy 2). The

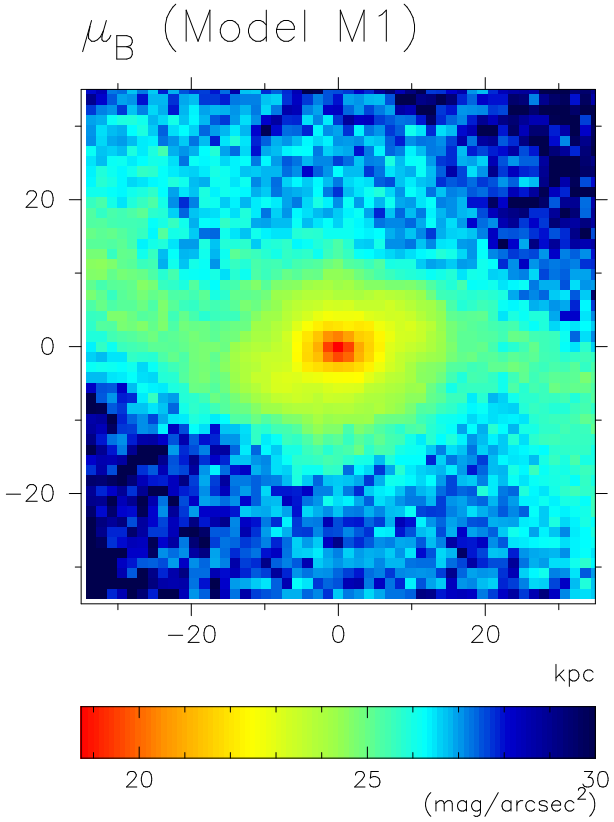

Figure 6. $B-$band surface brightness ($\mu_{\rm B}$) distribution at the epoch of the maximum AR in the standard model (M1).

mass of the forming elliptical is $\sim 3M_{\rm d}$ corresponding to $\sim 1.8\times10^{11}\mathrm{M}_{\odot}$ and the final combined mass of SMBH1 and SMBH2 is $7.7\times10^{8}\mathrm{M}_{\odot}$. Therefore, the remnant elliptical of this model shows $M_{\rm SMBH}/M_{\rm sph} = 4.3\times10^{-3}$, where $M_{\rm sph}$ is the total mass of the elliptical. This ratio of $M_{\rm SMBH}/M_{\rm sph}$ is reasonably consistent with the observed value of 0.006 (Magorrian et al. 1998). Given the fact that $M_{\rm SMBH}/M_{\rm sph} = 2.0\times10^{-3}$ for the model with no growth of SMBHs, the result shown in Figure 4 suggests that the growth of SMBHs during merging is quite important for elliptical galaxies formed by merging to show $M_{\rm SMBH}-M_{\rm sph}$ relation similar to the observed one (Magorrian et al. 1998).

Figure 5 describes the time evolution of projected mass densities of new stars ($\Sigma_{\rm ns}$)) and column densities ($\Sigma_{\rm g}$), which is a measure of the degree of dust extinction for a given metallicity (e.g., Binney & Merrifield 1998). Figure 5 clearly shows the significantly increased values of $\Sigma_{\rm ns}$ after $T \sim 1.8$ Gyr mean that SMBHs are surrounded by compact poststarburst populations formed during galaxy merging. The very large values of $\Sigma_{\rm g}$ around $T = 1.9$ Gyr mean that SMBHs (thus AGN) are heavily obscured by metal-enriched gas (thus dust).

Figure 6 shows the $B-$band surface brightness ($\mu_{\rm B}$) distribution of the merger at the epoch of maximum AR. Two disks are completely destroyed to form a spheroidal component by violent relaxation until this epoch, and only weak signs of tidal disturbance can be seen in its outer stellar halo. Owing to the low surface brightness outer halo components ($\mu_{\rm B} > 27$ mag arcsec^{-1}), this merger with a QSO-like activity can be classified morphologically as an E if it is located

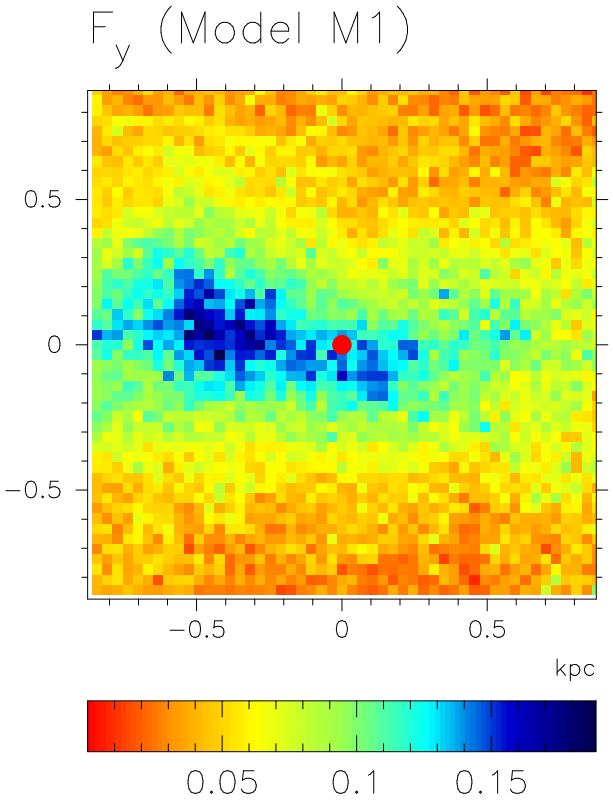

Figure 7. The 2D distribution of the mass fraction of new stars ($F_{\rm y}$) in the standard model (M1). The location of the SMBH1 is indicated by a red filled circle. Note that the SMBH is surrounded by young stellar populations.

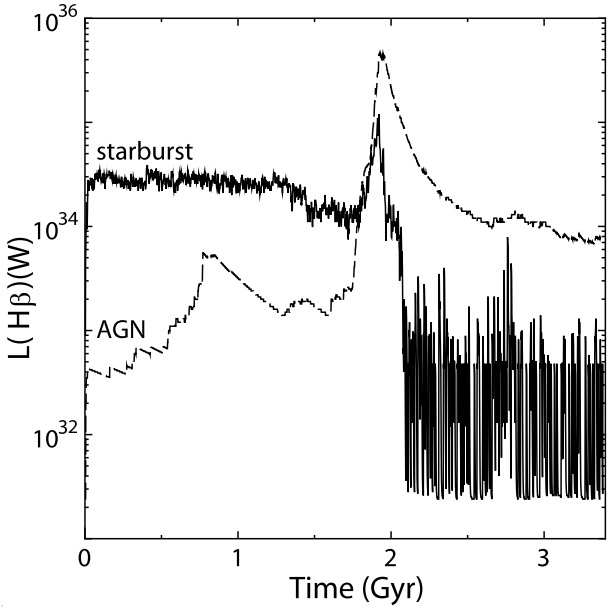

Figure 8. Time evolution of $L_{\rm H\beta}$ (in units of Watts) for the starburst component (solid line) and the AGN component (dashed) in the standard model. Note that the contribution from the AGN strengthens significantly around T=1.9 Gyr, when the merger becomes an AGN-dominated ULIRG.

at high redshift with $z > 1$ (e.g., Bekki et al. 1999 for morphological properties of high z starbursting mergers). This result suggests that *some intermediate- and high-redshifts QSO host galaxies with apparently spheroidal morphologies can be forming elliptical via dissipative major merger events.* This result accordingly appears to be consistent with an observational result (Floyd et al. 2004) that QSO hosts at $z \sim 0.4$ are massive bulge-dominated galaxies.

Figure 7 shows the two dimensional (2D) distribution of $F_{\rm y}$ of the merger at the epoch of maximum AR, where $F_{\rm y}$ is the mass fraction of new stars (as a proportion of the total number) in the central regions of the merger. This figure indicates that (1) the central SMBH (in the galaxy 1) can be surrounded by young starburst or poststarburst components in the central 1 kpc of the merger and (2) the location of the SMBH is however not necessarily coincident exactly with the location where most of the very young stellar components are formed in the final phase of merging. This difference in the locations of the SMBH and the starburst region does not stay significant, as the two SMBHs dynamically disperse the young compact starburst components when they become closer to each other. Most of the present major merger models show the coexistence of young starburst (or poststarburst) and AGN components in the central 1 kpc of mergers when morphological transformation is nearly completed.

We here stress that the derived coexistence of *moderately strong starburst* ($\dot{m}_{\rm sf} \approx 30 {\rm M}_{\odot}{\rm yr}^{-1}$) *and QSO-like AGN* ($\dot{m}_{\rm acc} \approx 3 {\rm M}_{\odot}{\rm yr}^{-1}$) is due partly to gas consumption by the growth of accretion disks and SMBHs. Our model with no gas accretion onto accretion disks and SMBHs (model M2) shows SFR of $\sim 640 {\rm M}_{\odot}{\rm yr}^{-1}$, which is significantly higher than that of the standard model (See the 7th and 8th columns in the table 1). These comparative experiments indicate that the presence of SMBHs that can swallow gas and input feedback energy can significantly influence SFRs in galaxy mergers.

Owing to rapid chemical enrichment from efficient star formation during starburst phases of galaxy merging, the stellar metallicities of stellar populations that are located within 100pc of SMBHs at the maximum AR (i.e. QSO phases) become as high as $2{\rm Z}_{\odot}$, where ${\rm Z}_{\odot}$ is the solar metallicity (=0.02). The mean ages of new stars around SMBHs is 0.85 Gyr for SMBH1 and 0.71 Gyr for SMBH2 at the maximum AR of the merger. Given the fact that Balmer absorption lines can become strong (thus show "E+A" spectra) ~ 1 Gyr after dusty starbursts (e.g., Bekki et al. 2001), the above results strongly suggest that SMBHs in AGN-dominated ULIRGs can be surrounded by metal-rich and young stellar populations with strong Balmer absorption lines. We discuss an evolutionary link between ULIRGs, QSOs, and E+A's later in §4.3.

3.1.2 Emission line properties

Figure 8 shows time evolution of $L_{\rm H\beta}$ separately for the starburst and AGN components. Although $L_{\rm H\beta}$ of the starburst is larger than that of the AGN in the early phases of galaxy merging ($T < 1.8$ Gyr), it becomes significantly smaller than that of the AGN when gas fuelling to the SMBHs becomes efficient ($T \sim 1.9$ Gyr). $L_{\rm H\beta}$ of the AGN component is always significantly larger than that of the starburst one after the coalescence of the two bulges: owing to very minor,

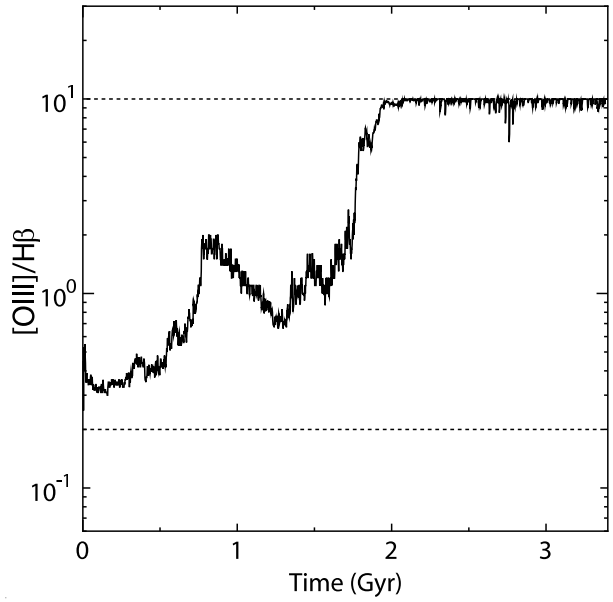

Figure 9. Time evolution of the emission line ratio of [O III]/Hβ in the galaxy merger of the standard model. Upper and lower (horizontal) dotted lines represent typical values of starburst and AGN, respectively. Note that as galaxy merging proceeds, the emission line ratio evolves from starburst-like one into AGN-like one.

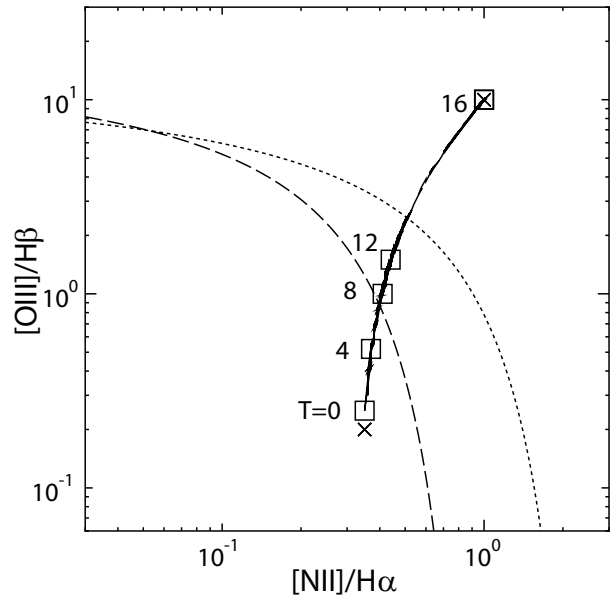

Figure 10. Time evolution of the galaxy merger in the standard model on the [O III]/Hβ-[N II]/Hα diagram. For clarity and comparison, only the results at selected epochs are described. The results at 5 time steps (in simulation units) are indicated by squares (T = 4, 8, 12, 16 correspond to 0.56, 1.13, 1.69, and 2.26 Gyr, respectively). The lower and upper crosses represent typical values for starbursts and AGN, respectively. Dotted and dashed lines represent the division between starbursts and AGN by Kewley et al. (2001) and Kauffmann et al. (2003b), respectively.

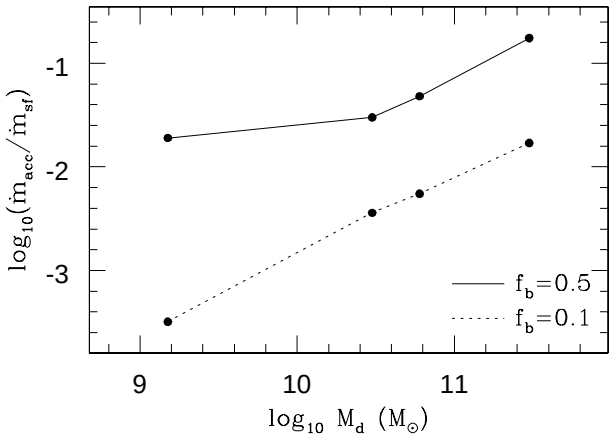

Figure 11. Dependences of $\dot{m}_{\rm acc}/\dot{m}_{\rm sf}$ on the initial disk masses ($M_{\rm d}$) for the two sets of models with $f_{\rm b} = 0.5$ (solid) and $f_{\rm b} = 0.1$ (dotted). Both $\dot{m}_{\rm acc}$ and $\dot{m}_{\rm sf}$ are estimated at the epochs of their maximum values.

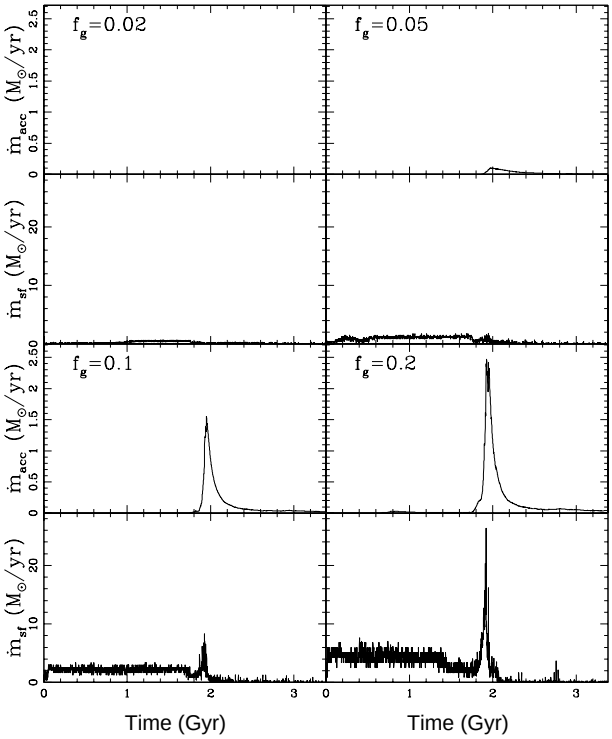

Figure 12. Time evolution of ARs ($\dot{m}_{\rm acc}$) and SFRs ($\dot{m}_{\rm sf}$) for four models with different gas mass fraction: $f_{\rm g} = 0.02$ (upper left), $f_{\rm g} = 0.05$ (upper right),$f_{\rm g} = 0.1$ (lower left), and $f_{\rm g} = 0.2$ (lower right).

sporadic star formation after galaxy merging, $L_{\rm H\beta}$ of the merger remnant is dominated by the weak AGN component. Figure 9 clearly demonstrates that the emission line ratio of [O III]/Hβ of the merger changes from the value typical for starbursts into that typical for AGN at $T \sim 1.9$ Gyr. These results are consistent with the result (in Figure 3) that $L_{\rm acc}/L_{\rm sb}$ becomes very high (> 100) at $T \sim 1.9$ Gyr.

Figure 10 shows the time evolution of the galaxy merger on the [O III]/Hβ-[N II]/Hα diagram, which is often used as a diagnostic for determining whether spectral properties of

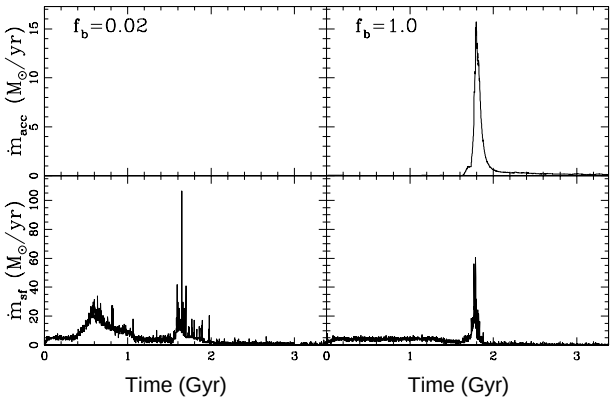

Figure 13. Time evolution of ARs ($\dot{m}_{\rm acc}$) and SFRs ($\dot{m}_{\rm sf}$) for two models with different bulge-to-disk-ratios: $f_{\rm b}$ = 0.02 (left), and $f_{\rm b}$ = 1.0 (right).

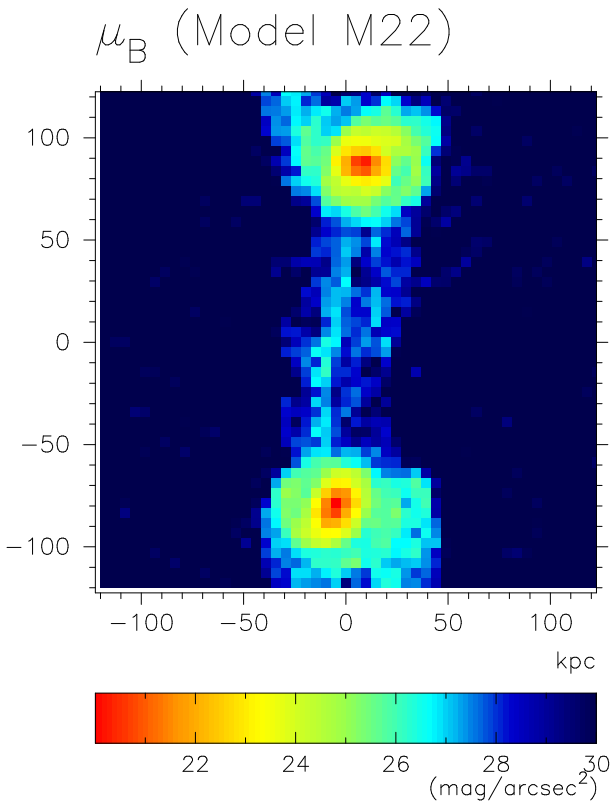

Figure 14. The same as Figure 6 but for the tidal interaction model (M22).

galaxies are dominated by starbursts or AGN (e.g., Baldwin, Phillips & Terlevich 1981; Veilleux & Osterbrock 1987; Kewley et al. 2001). We also plot on the Figure two lines that demarcate the locations of AGN- and starburst-dominated sources. The first (dashed) line is the "extreme starburst classification line" from Kewley et al (2001), a theoretically-derived upper limit for starburst models. The second (dotted) line comes from Kauffman et al (2003b), and is based on a large observational set of data from the Sloan Digital Sky Survey. Starburst spectra should reside below these lines, while AGN spectra should be found to the upper right. It is clear from Figure 10 that the merger evolves from the

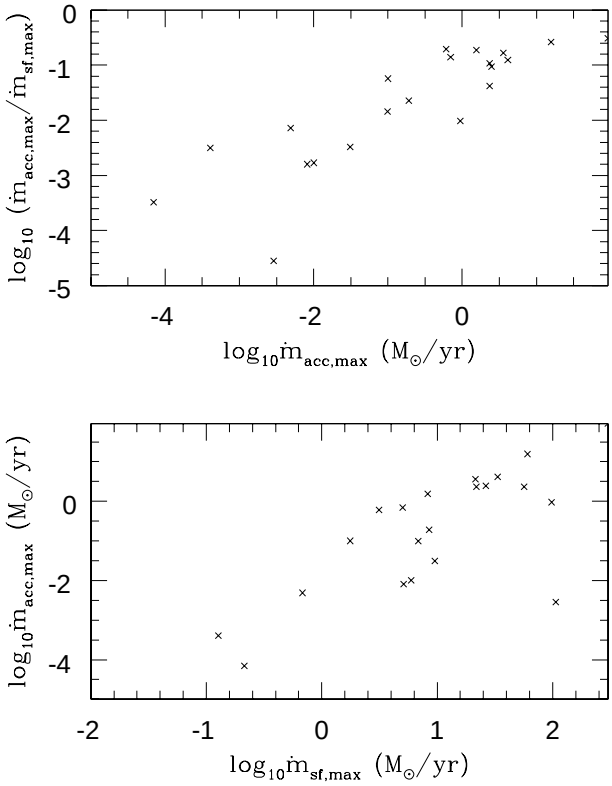

Figure 15. The Dependence of the ratio of maximum AR ($\dot{m}_{\rm acc,max}$) to maximum SFR ($\dot{m}_{\rm sf,max}$) on $\dot{m}_{\rm acc,max}$ (upper) and the dependence of $\dot{m}_{\rm acc,max}$ on $\dot{m}_{\rm sf,max}$ (lower) for the present 21 models.

middle of the starburst region toward the AGN-dominated region in the upper right.

The results in Figures 8, 9 and 10 clearly show that there is an evolutionary link between starburst and AGN in terms of the spectral properties of the merger. These results are consistent with the derived SFRs and ARs (e.g., Figures 2 and 3), furthermore demonstrating the capability of our new codes in correctly predicting spectroscopic properties of galaxy mergers with a coexistence of starbursts and AGN. Full discussions on emission and absorption line properties of (including spectral lines other than those discussed above, e.g., Hγ absorption line) of galaxy mergers will be given in our forthcoming papers (e.g., Bekki & Shioya 2005).

3.2 Parameter dependences

Although the numerical results on the coexistence of starbursts and AGN are similar for most of the merger models considered, the magnitudes of SFRs and ARs depend on $M_{\rm d}$, $f_{\rm g}$, $f_{\rm b}$, m_2, and orbital configuration of merging. We illustrate here the derived dependences and some physical correlations between SFRs and ARs in galaxy mergers.

3.2.1 $M_{\rm d}$

Figure 11 shows how the relative importance of starbursts and AGN in galactic nuclei of galaxy mergers depends on the masses of the progenitor disks. For two sets of models with different bulge-to-disk-ratio ($f_{\rm b}$ = 0.1 and 0.5),

$\dot{m}_{\rm acc}/\dot{m}_{\rm sf}$ is larger for larger $M_{\rm d}$, which means that more massive galaxy mergers are likely to be dominated by AGN rather than by starbursts. This is essentially because the interstellar gas that is radially transferred from outer parts of mergers can be consumed more by SMBHs than by starbursts owing to the larger initial masses of SMBHs (i.e. $M_{\rm SMBH} = 0.006 f_{\rm b} M_{\rm d}$) in more massive mergers. We discuss this result later (§4) in the context of the origin of ULIRGs.

3.2.2 $f_{\rm g}$

Figure 12 shows that maximum SFR and ARs in galaxy mergers with larger gas mass fraction ($f_{\rm g}$) are both higher compared to those with smaller gas mass fraction. This is because the total amount of gas transfered to the vicinity of SMBHs is larger for the mergers with larger $f_{\rm g}$ owing to a larger amount of gaseous dissipation in these. Figure 12 also shows that mergers with $f_{\rm g} < 0.1$ exhibit ARs much smaller than the $0.7{\rm M}_\odot{\rm yr}^{-1}$ required for QSO activity. These results suggest that $f_{\rm g}$ is one of key parameters that determine whether galaxy mergers show QSO activity in their nuclei. Irrespective of $f_{\rm g}$, the epoch of maximum SFR and that of maximum AR are nearly coincide with each other, which implies that coexistence of starbursts and AGN can be quite common phenomena in galaxy mergers.

3.2.3 $f_{\rm b}$

Figure 13 describes the time evolution of SFRs and ARs for the two extreme cases of mergers with $f_{\rm b} = 0.02$ (nearly bulge-less spiral progenitor) and $f_{\rm b} = 1.0$ (early-type M31-like spiral progenitor). It is clear from this figure that maximum accretion rates at the epoch of maximum SFRs are quite different to each other in these two cases: maximum $\dot{m}_{\rm acc}$ is $1.6 \times 10{\rm M}_\odot{\rm yr}^{-1}$ for $f_{\rm b} = 1.0$ and $3.0 \times 10^{-3}{\rm M}_\odot{\rm yr}^{-1}$ for $f_{\rm b} = 0.02$. This is due to the fact that the initial $M_{\rm SMBH}$ can determine ARs in the present model for the formation and the growth of accretion disks. Figure 13 also shows that there is little difference in the maximum SFR between the two models. This result suggests that $f_{\rm b}$ is also a key parameter which can determine whether galactic nuclei of mergers can be dominated by starbursts or AGN.

The accretion radius ($R_{\rm B}$) within which gas clouds can be converted into accretion disks is initially small for small SMBHs in the model (M19) with $f_{\rm b} = 0.02$, owing to the adopted assumption of $R_{\rm B} \propto M_{\rm SMBH}$. Therefore, gas clouds have to lose a larger amount of angular momentum (with respect to SMBHs) to reach $R_{\rm B}$ during merging. As a result, gas is consumed by star formation rather than by the growth of accretion disks around SMBHs. Thus, the AR is significantly smaller compared with other major merger models with bigger bulges. It should however be stressed here that if we relax the assumption of $R_{\rm B} \propto M_{\rm SMBH}$, the AR in the model M19 can also reach high values.

Thus it should be stressed that it depends on the models of accretion radius ($R_{\rm B}$ dependent on $M_{\rm SMBH}$ or not) whether initially small MBHs (with masses of $\sim 10^6{\rm M}_\odot$ in the models with small $f_{\rm b}$) can grow to become SMBHs (with masses of $\sim 10^6{\rm M}_\odot$). Although both previous models (e.g., Springel et al. 2005b) and the present one assume a relation between $R_{\rm B}$ and $M_{\rm SMBH}$, it is not so clear (theoretically) whether there really exists such a relation around SMBHs in galaxies. It would be therefore safe to say that future very high-resolution numerical simulations, in which a $R_{\rm B} - M_{\rm SMBH}$ relation is more self-consistently determined from sub-pc scale gas dynamics around SMBHs, will provide a more robust prediction on this matter.

3.2.4 m_2

Both maximum SFRs and ARs depend strongly on m_2 such that they are higher in mergers with larger m_2 (See the 7th and 8th columns of the table 1 for the models M1, M13, and M14). This is because a larger amount of interstellar gas can be driven into the central regions of galaxy mergers owing to stronger tidal disturbance and the resultant larger amount of shock dissipation in mergers with larger m_2. $\dot{m}_{\rm acc}$ in minor (M13) and unequal-mass (M14) mergers are well below $1{\rm M}_\odot{\rm yr}^{-1}$, so that these merger remnants do not show QSO activity and thus may well be identified as low luminosity AGN. Since these minor and unequal-mass mergers ultimately become S0s whereas major mergers can become Es (Bekki 1998), S0s are more likely to show low luminosity AGN activity. These results also imply that there can be a correlation between AGN host morphological types (e.g, Es or S0s) and nonthermal luminosities of AGN.

The HSB minor merger model (M15) shows a significantly high AR ($\dot{m}_{\rm acc} = 0.2{\rm M}_\odot{\rm yr}^{-1}$) compared with the LSB counterpart M13 ($\dot{m}_{\rm acc} = 0.01{\rm M}_\odot{\rm yr}^{-1}$), which suggests that the compactness of the smaller galaxy in a minor merger is a key factor for gas fuelling to the central SMBHs. The reason for this high AR is that the smaller galaxy of the HSB model can not be destroyed by the larger galaxy until the final coalescence of the two galaxies so that it tidally disturbs the ISM of the larger galaxy more strongly and for a longer time and thus triggers more efficient gas fuelling.

3.2.5 Orbital configurations

No significant dependences of time evolution of SFRs and ARs on orbital configurations are found for a given set of parameters (See the 7th and 8th columns of table 1 for the models, M1, M10, M11, and M12). Typical SFRs and ARs are of the order of $10{\rm M}_\odot{\rm yr}^{-1}$ and $1{\rm M}_\odot{\rm yr}^{-1}$ respectively, in these major merger models. Given the derived m_2 dependences, these results suggest major merging ($m_2 > 0.3$) is one of requisite conditions for QSO formation.

3.2.6 Tidal interaction

Both SFRs and ARs can be significantly enhanced in tidal interaction models, however the degree of the enhancement is much less remarkable compared with major merger models. Major merger models with bigger bulges (i.e. larger $f_{\rm b}$) can show larger ARs, whereas tidal interaction models with bigger bulges do not show high ARs ($\sim 0.7{\rm M}_\odot{\rm yr}^{-1}$). This is because formation of strong stellar bars, which are the main drivers for gas fuelling to starbursts and AGN, can not be formed in the bigger bulge models (e.g., $f_{\rm b} = 0.5$). Thus, tidal interaction models show high ARs only when they involve smaller bulges and larger disk masses.

Figure 14 shows the 2D distribution of $\mu_{\rm B}$ in the tidal interaction model M22, with $M_{\rm d} = 3.0 \times 10^{11}{\rm M}_\odot$, $f_{\rm b} = 0.1$

, and $M_{\rm SMBH} = 0.012 M_{\rm b}$ at the epoch of its maximum AR ($2.4 {\rm M}_{\odot} {\rm yr}^{-1}$). Although we have investigated several representative tidal interaction models, only this tidal model with more massive SMBHs shows a sufficiently high AR ($> 0.7 {\rm M}_{\odot} {\rm yr}^{-1}$) to become a QSO. It is clear from Figure 14 that interacting galaxies with QSO activity can be identified as two galaxies. This is quite different from major merger models in which a merger with a QSO activity almost always shows a single elliptical morphology. Given the very limited range of parameters for tidal interaction models to show QSO activities, these results imply that, if they are formed by galaxy interaction and merging, (1) most of QSO hosts can be elliptical galaxies and (2) binary QSOs can be very rare.

This is borne out by observational results. Mortlock et al. (1999) found only 16 binary QSOs, and calculated an "activation radius" of between 50 and 100 kpc (cf. Figure 14). Assuming these were formed in a galaxy-galaxy collision, this implies that QSO formation occurs late in the collision process. A more recent survey of binary QSOs from the Sloan Digital Sky Survey and 2dF Quasar Redshift Survey (Hennawi et al. 2005) found 218 quasar pairs with separations $< 1 h^{-1}$Mpc, implying a binary fraction of ~ 1 in 1000.

3.2.7 Correlations between $\dot{m}_{\rm sf}$ and $\dot{m}_{\rm acc}$

Figure 15 shows that (1) there is a weak yet positive correlation between maximum SFRs ($\dot{m}_{\rm sf,max}$) and maximum ARs ($\dot{m}_{\rm acc,max}$) and (2) there is a clearer correlation between $\dot{m}_{\rm acc,max}$ and $\dot{m}_{\rm acc,max}/\dot{m}_{\rm sf,max}$. The above result (1) suggests that mergers with more pronounced starburst activities are likely to show more pronounced AGN ones. The result (2) suggests that mergers with more pronounced AGN activities are more likely to be dominated by AGN rather than starbursts. It should be however stressed here that if we plot $\dot{m}_{\rm sf}$ and $\dot{m}_{\rm acc}$ from data at every time step of all models (including non-AGN and non-starburst phases) in the same way as shown in Figure 10, the derived two correlations becomes rather weak. Thus the correlations can be held only for mergers with strong starbursts and AGN.

4 DISCUSSIONS

4.1 Relative importance of starbursts and AGN

Our numerical simulations have shown that galactic mass is a key factor in determining whether a forming early-type galaxy is dominated by starbursts or AGN. The present study has demonstrated that the bolometric luminosity ratio, $L_{\rm acc}/L_{\rm sf}$, is larger for galaxy mergers with larger initial disk masses ($M_{\rm d}$). An order of magnitude estimation can allow us to understand this result. For global galactic star formation, we adopt the Schmidt law, in which $\dot{m}_{\rm sf} \propto {\mu_{\rm g}}^{1.5}$, where $\mu_{\rm g}$ is the surface gas density of a disk. We also adopted the $M_{\rm d} - \mu_{\rm s}$ relation (Kauffman et al. 2003b) in the present study. Therefore $L_{\rm sf}$ can be approximated as:

$$L_{\rm sf} \propto \dot{m}_{\rm sf} \propto {\mu_{\rm g}}^{1.5} \propto {M_{\rm d}}^{0.75}, \quad (16)$$

for $\mu_{\rm g} \propto \mu_{\rm s}$ in the present models with radially constant gas mass fraction. On the other hand, $L_{\rm acc}$ can be approximated as:

$$L_{\rm acc} \propto \dot{m}_{\rm acc} \propto \dot{m}_{\rm Edd} \propto M_{\rm SMBH} \propto M_{\rm b} \propto M_{\rm d} \quad (17)$$

for a given bulge-to-disk-ratio ($f_{\rm b}$). Equation 16 and 17 lead us to derive the following relation:

$$\frac{L_{\rm acc}}{L_{\rm sf}} \propto \frac{\dot{m}_{\rm acc}}{\dot{m}_{\rm sf}} \propto {M_{\rm d}}^{0.25}. \quad (18)$$

This relation suggests that more luminous forming early-type galaxies via galaxy merging are likely to be dominated by AGN rather than by starbursts, if merger progenitor disks contain a sufficient amount of gas for fuelling.

Although the above analytically derived relation of $\frac{\dot{m}_{\rm acc}}{\dot{m}_{\rm sf}} \propto {M_{\rm d}}^{0.25}$ is qualitatively consistent with the simulations shown in in Figure 11, it is significantly shallower than those derived in the simulations ($\frac{\dot{m}_{\rm acc}}{\dot{m}_{\rm sf}} \propto {M_{\rm d}}^{0.95}$ for $f_{\rm b} = 0.1$ and $\frac{\dot{m}_{\rm acc}}{\dot{m}_{\rm sf}} \propto {M_{\rm d}}^{0.38}$ for $f_{\rm b} = 0.5$; See Figure 11). The origin of this difference might well be closely associated with the fact that suppression of star formation from AGN feedback (which can enhance the relative importance of accretion-power-induced activity in galactic nuclei) is not explicitly considered in the above analytical arguments.

It is currently less feasible to prove the above mass dependence based on the comparison between the simulation results and observations, because most of previous observations focused on correlations between nuclear activities and the Hubble morphological types (e.g., Mouri & Taniguchi 2004). It may well be an observationally difficult task to estimate *separately* $\dot{m}_{\rm sf}$ and $\dot{m}_{\rm acc}$ from emission line properties of galactic nuclei for determining $L_{\rm acc}/L_{\rm sf}$. We however suggest that future statistical studies on $L_{\rm acc}/L_{\rm sf}$ and its dependence on galactic masses are worthwhile, because they can prove an example of mass-dependent evolution of galaxies.

4.2 What powers ULIRGs ?

It has been a longstanding, remarkable problem what dominate the luminosities of ULIRGs since many observational studies with different wavelengths revealed possible evidences for both starbursts and AGN in ULIRGs (e.g., Sanders & Mirabel 1996; Lutz et al. 1998; Genzel et al. 1998; Tacconi et al. 2002). Based on a mid-infrared spectroscopic survey of 15 ULIRGs by ISO (Infrared Space Observatory, Genzel et al. (1998) revealed that there is no obvious trend for the AGN component to dominated in the most advanced mergers. Lutz et al (1998) investigated the ratio of the 7.7 μm PAH (polycyclic aromatic hydrocarbon) emission feature to the local continuum for 60 ULIRGs and found that only about 15% of ULIRGs at luminosities below $2 \times 10^{12} L_{\odot}$ are powered by AGN.

Our simulations have demonstrated that (1) initial galactic masses can be one of primarily important parameters that determine the relative importance of starbursts and AGN in galaxy mergers and (2) more massive galaxy mergers are likely to be dominated by AGN. Almost all ULIRGs show strongly disturbed morphological properties, which are the most likely to be clear signs of past major merger events (e.g., Sanders et al. 1988). A logical conclusion of these theoretical and observational results is that if ULIRGs are more massive then they are likely to be dominated by AGN. Figure 11 suggests that galaxy mergers with their progenitor disk masses higher than $\approx 10^{11} M_{\odot}$ and bigger bulges can

become ULIRGs with AGN. Recently Tacconi et al. (2002) have investigated structural and kinematical parameters of ULIRGs and found that ULIRGs are not so massive/bright as giant ellipticals. This result, combined with our simulations, suggests that ULIRGs are, *on average*, dominated by starbursts rather than AGN. This suggestion is broadly consistent with the observational results by Lutz et al. (1998) that about 80% of ULIRGs are found to be predominantly powered by starbursts. It is however not so clear why galaxy mergers between less luminous late-type galaxies are more likely to occur than those between more luminous ones at lower redshifts.

4.3 Evolutionary link between ULIRG, QSOs, Q+A's, and E+A's ?

Although the relative importance of starbursts and AGN in ULIRGs has been observationally suggested to be different between different ULIRGs (e.g., Genzel et al. 1998; Lutz et al. 1998), a significant fraction of ULIRGs have been suggested to contain starburst components (e.g., Farrah et al. 2003). These observational results raise the following question: Are there any evolutionary links between ULIRGs and galaxies with "E+A" spectra indicative of poststarburst populations (e.g., A-type stars) ? This question may well be quite timely and important, given the fact that physical properties of E+A's are now being extensively investigated for a large number of E+A samples derived by wide field surveys (e.g., Blake et al. 2004; Goto et al. 2003) and by 8m-class ground telescopes with multi-object spectrograph (e.g., Pracey et al. 2004). Spectral signatures of poststarburst stellar populations in some QSOs (e.g., Canalizo & Stockton 2000; 2001) and in some ULIRGs (e.g., Poggianti & Wu 2000; Goto 2005) imply that there could be some close physical relationships between ULIRGs, QSOs, and E+A's. In the following discussion, QSOs with poststarburst spectra (i.e. strong Balmer absorption lines) are referred to as "Q+A's" just for convenience.

The present simulations have demonstrated that SMBHs of galaxy mergers can be surrounded by circumnuclear, compact, and young poststarburst populations when ARs onto SMBHs are high. This result implies that if the Balmer absorption lines are not significantly diluted by Balmer emission lines from AGNs, spectral signatures of poststarburst populations can be detected in galaxy mergers. Based on these numerical results, we suggest the following two different evolutionary paths between mergers (Mer) and ellipticals (Es). For SB-dominated ULIRGs that are formed by merging either between less luminous disks or between disks with smaller bulges, strong Balmer absorption lines can be detectable owing to less significant dilution of the absorption lines by emission lines from weaker AGN components. Therefore the evolutionary path could be;

$Mer \Rightarrow ULIRGs \Rightarrow E + A's \Rightarrow Es$.

For AGN-dominated ULIRGs that are formed by merging between more massive disks with prominent bulges, the evolutionary path could depend on whether the lifetimes of QSOs are shorter than the lifetimes of A-type stars. The present simulations have shown that the lifetime of QSOs (defined as the duration within which $\dot{m}_{\rm acc}$ is higher than 0.7 $M_\odot$) is an order of ~ 0.1 Gyr (See Hopkins et al. 2005 for possible luminosity dependent QSO lifetimes). The dilution of the Balmer absorption lines by AGN emission can be significant in the very strong AGN phases so that the absorption lines can not be detected so easily. The absorption lines might well be detectable either when intrinsic AGN luminosities become significantly smaller or when AGN are observed as type II (i.e. viewed from the edge of the surrounding dusty torus). Therefore there can be the following evolutionary path:

$Mer \Rightarrow ULIRGs \Rightarrow QSOs \Rightarrow (Q + A's) \Rightarrow E + A's \Rightarrow Es$.

Probably, QSOs that experienced stronger starbursts in the gas fuelling (thus growth) processes of SMBHs are more likely to have detectable Balmer absorption lines. It is also reasonable to claim that strong Balmer absorption lines are more likely to be detected in type 2 Seyfert than in type 1 owing to the less amount of dilution of stellar light by emission from hidden broad line regions of type 2 Seyfert (with weaker emission lines due to dusty torus around AGN). We plan to investigate this point more quantitatively by numerical simulations and compare the results with already existing observational results (e.g., Kauffmann et al. 2003a; Cid Fernandes et al. 2004).

As shown in the present chemodynamical study, the metallicities of stellar populations around SMBHs in galaxy mergers become very high ($> 2Z_\odot$) owing to rapid chemical enrichment associated with starbursts during galaxy merging. Furthermore, as a natural result of chemical evolution, the stellar metallicities around SMBHs are higher in the later phase of galaxy merging. These results imply that stellar populations in later AGN phases (e.g., QSOs and Liners) are more likely to be more metal-rich than those in earlier starburst phases for galaxy mergers with starbursts and AGN. Our previous chemodynamical simulations suggested that the abundance ratio of [Mg/Fe] after strong starburst of galaxy mergers can be significantly larger than the solar value due to the dominant contribution of Type II supernovae (Bekki & Shioya 1999). Therefore we suggest that *QSOs with younger poststarburst populations can show large [Mg/Fe] ratios if QSOs are evolved from ULIRGs formed by galaxy mergers.*

4.4 Pair vs multiple mergers in ULIRGs formation.

The present study has investigated mergers between two disk galaxies and thereby demonstrated that ULIRGs can be formed in the very late phase of galaxy merging when two galaxies nearly complete their merging. Thus the present model can be more relevant to ULIRGs with single cores: The presence of ULIRGs with multiple cores observed in some ULIRGs (e.g., Borne et al. 2000; Colina et al. 2001; Bushouse et al. 2002) can not be simply explained by the present pair merger models (Taniguchi & Shioya 1998). Previous numerical simulations showed that (1) a compact group of galaxies can be transformed into an elliptical galaxy through multiple merging of the group member galaxies (Barnes 1989; Weil & Hernquest 1996), (2) repetitive and multiple starbursts can be triggered by multiple merging of disk galaxies (Bekki 2001), and (3) the origin of metal-poor, hot gaseous halo of field giant ellipticals can be closely associated with tidal stripping of metal-poor gas in multiple mergers (Bekki 2001). However, previously nu-

merical studies did not calculate the accretion rates onto SMBHs and the SEDs in multiple mergers so that they could not provide any theoretical predictions as to (1) whether multiple mergers can become AGN-dominated ULIRGs or starburst-dominated ones, (2) in what physical conditions starbursts and AGN can be obscured heavily enough to become ULIRGs emitting almost all energy in infrared bands, and (3) what is the dynamical fate of multiple SMBHs fallen into the central regions of the remnants of multiple mergers.

Thus we plan to investigate the above questions based on more sophisticated, higher-resolution simulations that allow us to study both dynamical evolution of multiple SMBHs and gas accretion onto the SMBHs. The results of these future simulations, combined with those of the present study, will allow us to (1) investigate what types of compact groups (e.g., spiral-rich groups) can become starburst-dominated ULIRGs or AGN-dominated ones (or much less luminous infrared galaxies) in their conversion processes into field elliptical galaxies via multiple galaxy merging and (2) discuss statistics of the observed morphological properties (e.g., single or multiple cores) of ULIRGs (e.g., Murphy et al. 1996; Zheng et al. 1999; Borne et al. 1999; 2000; Colina et al. 2001; Cui et al. 2001; Bushouse et al. 2002; Goto 2005). These simulations will also help us to understand physical relationships between compact group of galaxies, multiple mergers, ULIRGs with hot gaseous halos (Xia et al. 2002; Huo et al. 2004), QSOs with companion galaxies (Stockton & Ridgway 1991; Disney et al. 1995; Hutchings & Morris 1995; Bahcall et al. 1997), "fossil group" with the central giant ellipticals (e.g., Ponman et al. 1994; Jones et al. 2003).

5 CONCLUSIONS

We have numerically investigated both SFRs and ARs in forming ULIRGs via gas-rich galaxy merging in an self-consistent way. Dependences of the time evolution of SFRs and ARs on model parameters are mainly investigated. We summarize our principle results as follows:

(1) ULIRGs powered by AGN can be formed by major merging between luminous, gas-rich disk galaxies with prominent bulges containing SMBHs owing to the efficient gas fuelling ($\dot{m}_{\rm acc} > 1{\rm M}_{\odot}$ yr^{-1}) to the SMBHs. AGN in these ULIRGs can be surrounded by compact poststarburst stellar populations (e.g., A-type stars). These results suggest that ULIRGs and QSOs can show strong Balmer absorption lines.

(2) ULIRGs powered by starbursts with $\dot{m}_{\rm sf} \sim 100{\rm M}_{\odot}$ yr^{-1} can be formed by merging between gas-rich disk galaxies with small bulges having the bulge-to-disk-ratio ($f_{\rm b}$) as small as 0.1. As long as the accretion radii ($R_{\rm B}$) of SMBHs are proportional to the masses of the SMBHs, galaxy mergers with smaller bulges are more likely to become starburst-dominated ULIRGs (i.e., they can not show AGN activity owing to a smaller amount of gas accretion onto the SMBHs).

(3) The relative importance of starbursts and AGN can depend on physical properties of merger progenitor disks, such as $f_{\rm b}$, gas mass fraction, and total masses. For example, more massive galaxy mergers are more likely to become AGN-dominated ULIRGs.

(4) For most models, major mergers can become ULIRGs powered either by starbursts or by AGN, when the two bulges finally merge. Interacting disk galaxies can become ULIRGs with well separated two cores (> 20kpc) at their pericenter only when they are very massive and have small bulges. These suggest that it is highly unlikely for interacting/merging pair of galaxies to become ULIRGs with double/multiple nuclei. We note, however, the results of Veilleux et al (2002), who found that about 7% of ULIRGs in their sample have nuclear separations in excess of 20kpc. This may suggest that ULIRGs can be formed via alternate routes to the major mergers examined herein.

(5) Irrespectively of models, interacting/merging galaxies show the highest accretion rates onto the central SMBHs and the resultant rapid growth of the SMBHs, when their star formation rates are very high.

(6) ARs can become high ($1{\rm M}_{\odot}{\rm yr}^{-1}$) enough to show QSO-like activities ($L_{\rm bol} \approx 10^{12}{\rm L}_{\odot}$) mostly in major mergers between massive disk galaxies with remarkable bulges. ARs however can not reach the required rates for QSOs ($\dot{m}_{\rm acc} \approx 0.7{\rm M}_{\odot}{\rm yr}^{-1}$) in minor and unequal-mass mergers that form S0s. These results therefore imply that only forming elliptical via major mergers can show QSO-like activities whereas forming S0s (or early-type spirals with big bulges) via minor and unequal-mass merging show low luminosity AGN (e.g., type 1/2 Seyfert).

(7) Maximum ARs ($\dot{m}_{\rm acc,max}$) can correlate with maximum SFRs ($\dot{m}_{\rm sf,max}$) in the sense that galaxy mergers with higher $\dot{m}_{\rm sf,max}$ are likely to show higher $\dot{m}_{\rm acc,max}$. This suggests that mergers and ULIRGs with more pronounced AGN activities are likely to show stronger starburst components in their nuclei. The correlations can be discussed in the context of recent observational results (e.g., Goto 2005) on correlations between infrared luminosities of ULIRGs, star formation rates, and AGN luminosities (measured from [OIII] emission lines).

(8) The ratio of $\dot{m}_{\rm acc,max}$ to $\dot{m}_{\rm acc,sf}$ can correlate with $\dot{m}_{\rm acc,max}$ in the sense that galaxy mergers with higher $\dot{m}_{\rm acc,max}$ are likely to show higher $\dot{m}_{\rm acc,max}/\dot{m}_{\rm sf,max}$. This implies that merger and ULIRGs with higher AGN (thus total) luminosities are likely to be dominated by AGN rather than by starbursts. This result can be also consistent with recent results on AGN fraction as a function of infrared luminosities of galaxies (e.g., Goto 2005).

(9) There could be evolutionary links between ULIRGs, Q+A's, QSOs, and E+A's. Galaxy mergers between less massive disks are more likely to evolve from starburst-dominated ULIRGs into E+As without experiencing QSO phases, whereas those between more massive disks with prominent bulges can evolve from AGN-dominated ULIRGs, to QSOs (and/or Q+A's), and finally to E+A's, if the lifetimes of QSOs are as short as $\sim$ 0.1 Gyr. Removal of gas reservoir for star formation via supernovae and AGN feedback could be essentially important for the above evolutionary links.

(10) Time evolution of emission line properties of galaxies with starbursts and AGNs is investigated based on SFRs and ARs derived from chemodynamical simulations. For example, simulated mergers are demonstrated to evolve from those with smaller [O III]/Hβ (starburst-dominated) to those with larger [O III]/Hβ (AGB-dominated). It is suggested that strong Balmer absorption lines are more likely to be detected in type 2 Seyfert than in type 1 owing to the less amount of

dilution of stellar light by emission from hidden broad line regions of type 2 Seyfert. Direct comparison between the predicted spectrophotometric properties of galaxy mergers with dusty starbursts and AGNs and the corresponding observations will be done in our forthcoming papers.

ACKNOWLEDGMENTS

We are grateful to the referee for valuable comments, which contribute to improve the present paper. KB acknowledges the financial support of the Australian Research Council throughout the course of this work. The numerical simulations reported here were carried out on GRAPE systems kindly made available by the Astronomical Data Analysis Center (ADAC) at National Astronomical Observatory of Japan (NAOJ).

REFERENCES

Armus, L., et al. 2004, ApJS, 154, 178
Baldwin, J. A., Wampler, E. J., Burbridge, E. M., 1981, 243, 76
Barger A. J., Cowie, L. L., Sanders, D. B., Fulton, E., Taniguchi, Y., Sato, Y., Kawara, K., Okuda, H. 1998, Nat, 394, 248
Bahcall, J. N., Kirhakos, S., Saxe, D. H., Schneider, D. P., 1997, ApJ, 479, 642
Barnes, J. E., 1989, Nat, 338, 123
Bekki, K. 1995, MNRAS, 276, 9
Bekki, K. 1998, ApJ, 502, L133
Bekki, K. 1999, ApJ, 510, L15
Bekki, K. 2000, ApJ, 545, 753
Bekki, K., Noguchi, M. 1994, A&A, 290, 7
Bekki, K., Shioya, Y. 1998, ApJ, 497, 108
Bekki, K., Shioya, Y. 1999, ApJ, 513, 108
Bekki, K., Shioya, Y. 2000, ApJ, 542, 201
Bekki, K., Shioya, Y. 2001, ApJS, 134, 241
Bekki, K., Shioya, Y., Tanaka, I. 1999, ApJ, 520, L99
Bekki, K., Shioya, Y., Couch, W. J. 2001, ApJ, 547, L17
Binney, J., & Tremaine, S. 1987 in Galactic Dynamics, Princeton; Princeton Univ. Press.
Binney, J., Merrifield, M., 1998, Galactic Astronomy, Princeton University Press,
Blain, A. W., Smail, I., Ivison, R. J., Kneib, J.-P., 1999, MNRAS, 302, 632
Blake, C., et al. 2004, MNRAS, 355, 713
Bondi, H., 1952, MNRAS, 112, 195
Borne, K. D., Bushouse, H., Colina, L., Lucas, R. A., Baker, A., Clements, D., Lawrence, A., Oliver, S., Rowan-Robinson, M., 1999, Ap&SS 266, 137
Borne, K. D., Bushouse, H., Lucas, R. A., Colina, L., 2000, ApJ, 529, L77
Bushouse, H. A., Borne, K. D., Colina, L., Lucas, R. A., Rowan-Robinson, M., Baker, A. C., Clements, D. L., Lawrence, A., Oliver, S., 2002, ApJS, 138, 1
Canalizo, G., Stockton, A., 2000, ApJ, 528, 201
Canalizo, G., Stockton, A., 2001, ApJ, 555, 719
Cid Fernandes, R., Gu, Q., Melnick, J., Terlevich, E., Terlevich, R., Kunth, D., Rodrigues L. R., Joguet, B., 2004, MNRAS, 355, 273
Clements, D. L., Sutherland, W. J., Saunders, W., Efstathiou, G. P., McMahon, R. G., Maddox, S., Lawrence, A., & Rowan-Robinson, M. 1996, MNRAS, 279, 459
Colina, L., Arribas, S., Monreal-Ibero, A., 2005, ApJ, 621, 725
Colina, L., Borne, K., Bushouse, H., Lucas, R. A., Rowan-Robinson, M.,; Lawrence, A., Clements, D., Baker, A., Oliver, S. 2001, ApJ, 563, 546
Cui, J., Xia, X.-Y., Deng, Z.-G., Mao, S., Zou, Z.-L., 2001, AJ, 122, 63
Di Matteo, T., Springel, V., Hernquist, L., 2005, Nat, 433, 604
Disney, M. J., Boyce, P. J., Blades, J. C., Boksenberg, A., Cane, P., Deharveng, J. M., Macchetto, F., Mackay, C. D., Sparks, W. B., Phillipps, S., 1995, Nat, 376, 150
Dopita, M. A., Reuland, M., Groves, B., Röttgering, H., van Breugel, W., 2006, AN, 327, 155
Faber, S. M., Jackson, R. E. 1976, ApJ, 204, 668
Farrah, D., Afonso, J., Efstathiou, A., Rowan-Robinson, M., Fox, M., Clements, D., 2003, MNRAS, 343, 585
Floyd, D. J. E., Kukula, Marek J., Dunlop, J. S., McLure, R. J., Miller, L., Percival, W. J., Baum, S. A., O'Dea, C. P., 2004, MNRAS, 355, 196
Frank, J., King, A., Raine, D. J., 2002, Accretion Power in Astrophysics, Cambridge, UK, Cambridge University Press.
Gao, Y., Solomon, P. M., 1999, ApJ, 512, L99
Genzel, R. et al. 1998, ApJ, 498, 579
Gerritsen, J. P. E., & Icke, V. 1999, in Galaxy interaction at low and high redshift ed. J. E. Barnes and D. B. Sanders, IAU symp. 186, p213
Goto, T., et al., 2003, PASJ, 55, 739
Goto, T., 2005, MNRAS, 360, 322
Hausman, M. A., Roberts, W. W. Jr., 1984, ApJ, 282, 106
Hoyle, F., Lyttleton, R. A., 1941, MNRAS, 101, 227
Hennawi, J. F. et al., 2005, ApJ, submitted, astro-ph/0504535
Hernquist, L., 1990, ApJ, 356, 359
Hopkins, P. F., Hernquist, L., Cox, T. J., Di Matteo, T., Robertson, B., Springel, V., 2005, ApJ, 630, 716
Hutchings, J. B., Morris, S. C., 1995, AJ, 109, 1541
Huo, Z. Y., Xia, X. Y., Xue, S. J., Mao, S., Deng, Z. G., 2004, ApJ, 611, 208
Imanishi, M., Terashima, Y., 2004, AJ, 127, 758
Iwasawa, K., Sanders, D. B., Evans, A. S., Trentham, N., Miniutti, G., Spoon, H. W. W., 2005, MNRAS, 357, 565
Jones, L. R., Ponman, T. J., Horton, A., Babul, A., Ebeling, H., Burke, D. J., 2003, MNRAS, 343, 627
Jonsson, P., Cox, T. J., Primack, J. R., 2005, in The Spectral Energy Distributions of Gas-Rich Galaxies: Confronting Models with Data, Edited by Cristina C. Popescu and Richard J. Tuffs. AIP Conference Proceedings, Vol. 761, p320
Kauffmann, G. et al. 2003a, MNRAS, 346, 1055
Kauffmann, G. et al. 2003b, MNRAS, 341, 54
Kennicutt, R. C., Jr., Keel, W. C., Blaha, C. A., 1989, AJ, 97, 1022
Kennicutt, R. C., 1998, ARA&A, 36, 189
Kewley, L. J., Dopita, M. A., Sutherland, R. S., Heisler, C. A., Trevena, J., 2001, ApJ, 556, 121
Kraemer, S. B., George, I. M., Crenshaw, D. M., Gabel, J. R., 2004, ApJ, 607, 794

Larson, R. B., 1981, MNRAS, 194, 809
Liu, F. K., 2004, MNRAS, 347, 1357
Lutz, D., Spoon, H. W. W., Rigopoulou, D., Moorwood, A. F., M., & Genzel, R. 1998, ApJ, 505, L103
Magorrian, J., 1998, AJ, 115, 2285
Mihos, J. C., Hernquist, L., 1994, ApJ, 431, L9
Mihos, J. C., Hernquist, L., 1996, ApJ, 464, 641
Mortlock, D. J., Webster, R. L., & Francis, P. J., 1999, MNRAS, 309, 836
Mouri, H., Taniguchi, Y., 2004, ApJ, 605, 144
Murphy, T. W., Jr., Armus, L., Matthews, K., Soifer, B. T. Mazzarella, J. M., Shupe, D. L., Strauss, M. A., Neugebauer, G., 1996, AJ, 111, 1025
Navarro, J. F., Frenk, C. S., White, S. D. M.1996, ApJ, 462, 563
Olson, K. M., Kwan, J. 1990, ApJ, 361, 426
Poggianti, B. M., Wu, H. 2000, ApJ, 529, 157
Ponman, T. J., Allan, D. J., Jones, L. R., Merrifield, M., McHardy, I. M., Lehto, H. J., Luppino, G. A., 1994, Nat, 369, 462
Pracy, M. B., Couch, W. J., Blake, C., Bekki, K., Harrison, C., Colless, M., Kuntschner, H., de Propris, R., 2005, MNRAS, 359, 1421
Rees, M., 1984, ARA&A, 22, 471
[Sanders et al. 1988]ss88 Sanders, D. B., Soifer, B. T., Elias, J. H., Modore, B. F., Mattehews, K., Neugbauer, G., Scoville, N. Z. 1988a, ApJ, 325, 74
Sanders, D. B., & Mirabel, I. F. 1996, ARA&A, 34, 749
Sanders, D. B., Kim, D.-C., Mazzarella, J. M., Surace, J. A., & Jensen, J. B. 1999, preprint (astro-ph/9911391)
Schmidt, M. 1959, ApJ, 344, 685
Schwarz, M. P. 1981, ApJ, 247, 77
Scoville, N. Z., Evans, A. S., Dinshaw, N., Thompson, R., Rieke, M., Schneider, G., Low, F. J., Hines, D., Stobie, B., Becklin, E., & Epps, H. 1998, ApJ, 492, L107
Scoville, N. Z., Evans, A. S., Thompson, R., Rieke, M., Hines, D., Low, F. J., Hines, D., Dinshaw, N., Surace, J. A., & Armus, L. 1999, preprint (astro-ph/9912246)
Shapiro, S. L., Teukolsky, S. A., 1983, Black holes, white dwarfs, and neutron stars: The physics of compact objects
Shioya, Y., Bekki, K., 1998, ApJ, 504, 42
Shioya, Y., Bekki, K., 2000, ApJ, 539, L29
Shioya, Y., Bekki, K., Couch, W. J., 2001, ApJ, 558, 42
Shioya, Y., Bekki, K., Couch, W. J., De Propris, R., 2001, ApJ, 565, 223,
Shioya, Y., Bekki, K., Couch, W. J., 2004, ApJ, 601, 654
Smail, I., Ivison, R. J., Blain, A. W., 1997, ApJ, 490, L5
Smail, I., Ivison, R. J., Blain, A. W., Kneib, J.-P. 1998, ApJ, 507, L21
Smail, I., Ivison, R. J., Kneib, J.-P., Cowie, L. L., Blain, A. W., Barger, A. J., Owen, F. N., Morrison, G., 1999, MNRAS, 308, 1061
Smith, H. E., Lonsdale, C. J., Lonsdale, C. J., 1998, ApJ, 493, L17
Soifer, B. T., Sanders, D. B., Neugebauer, G., Danielson, G. E., Lonsdale, Carol J., Madore, B. F., Persson, S. E., 1986, ApJ, 303, L41
Solomon, P. M., Downes, D., Radford, S. J. E., 1992, ApJ, 387, L55
Springel, V., Di Matteo, T., Hernquist, L., 2005a, ApJ, 620, L79
Springel, V., Di Matteo, T., Hernquist, L., 2005b, MNRAS, 361, 776
Stockton, A., Ridgway, S. E., 1991, AJ, 102, 488
Sugimoto, D., Chikada, Y., Makino, J., Ito, T., Ebisuzaki, T., & Umemura, M. 1990, Nat, 345, 33
Surace, J. A., Sanders, D. B., Evans, A. S., 2000, ApJ, 529, 170
Tacconi, L. J., Genzel, R., Lutz, D., Rigopoulou, D., Baker, A. J., Iserlohe, C., Tecza, M., 2002, ApJ, 580, 73
Taniguchi, Y., Shioya, Y., 1998, ApJ, 501, L167
Thornton, K., Gaudlitz, M., Janka, H.-Th., Steinmetz, M., 1998, ApJ, 500, 95
Trentham, N., Kormendy, J., Sanders, D. B., 1999, AJ, 117, 2152
Veilleux, S., Osterbrock, D. E., 1987, ApJS, 63, 295
Veilleux, S, Kim, D.-C., Sanders, D. B., 1999, ApJ, 522, 113
Veilleux, S. K., Kim, D.-C., Sanders, D. B., 2002, ApJS, 143, 315
Wielen, R. 1977, A&A, 60, 263
Xia, X. Y., Xue, S. J., Mao, S., Boller, Th., Deng, Z. G., Wu, H., 2002, ApJ, 564, 196
Zheng, Z., Wu, H., Mao, S., Xia, X.-Y., Deng, Z.-G., Zou, Z.-L., 1999, A&A, 349, 735

This figure "f1.jpg" is available in "jpg" format from:

http://arXiv.org/ps/astro-ph/0607349